

Presenting Climate Projection Ensembles as Mean and Reasonable Worst Case, with Application to EURO-CORDEX Precipitation

Stephen Jewson (✉ stephen.jewson@gmail.com)

London, UK <https://orcid.org/0000-0002-6011-6262>

Gabriele Messori

Uppsala Universitet

Giuliana Barbato

CMCC: Centro Euro-Mediterraneo sui Cambiamenti Climatici

Paola Mercogliano

CMCC: Centro Euro-Mediterraneo sui Cambiamenti Climatici

Jaroslav Mysiak

CMCC: Centro Euro-Mediterraneo sui Cambiamenti Climatici

Maximiliano Sassi

RMS Ltd

Research Article

Keywords: climate projection, ensemble mean, worst-case, DCA, EURO-CORDEX, precipitation

Posted Date: May 11th, 2021

DOI: <https://doi.org/10.21203/rs.3.rs-494689/v1>

License: © ⓘ This work is licensed under a Creative Commons Attribution 4.0 International License.

[Read Full License](#)

1 **Presenting Climate Projection Ensembles as Mean and Reasonable Worst Case, with Application to EURO-**
2 **CORDEX Precipitation**

3 Stephen Jewson¹, Gabriele Messori^{2,3}, Giuliana Barbato⁴, Paola Mercogliano⁴, Jaroslav Mysiak⁴, Maximiliano
4 Sassi⁵

5 ¹London, UK

6 ²Department of Earth Sciences and Centre of Natural Hazards and Disaster Science (CNDS), Uppsala University,
7 Uppsala, Sweden

8 ³Department of Meteorology and Bolin Centre for Climate Research, Stockholm University, Stockholm, Sweden

9 ⁴Euro-Mediterranean Center on Climate Change (CMCC) Foundation, Via Augusto Imperatore, 16, 73100, Lecce,
10 Italy

11 ⁵Risk Management Solutions Ltd, EC3R 7AG, London, UK

12 Corresponding author: Stephen Jewson (stephen.jewson@gmail.com)

13 **Abstract**

14 Users of ensemble climate projections have choices with respect to how they interpret and apply the ensemble. A
15 simplistic approach is to consider just the ensemble mean and ignore the individual ensemble members. A more
16 thorough approach is to consider every ensemble member, although for complex impact models this may be
17 unfeasible. Building on previous work in ensemble weather forecasting we explore an approach in-between these
18 two extremes, in which the ensemble is represented by the mean and a reasonable worst case. The reasonable
19 worst case is calculated using Directional Component Analysis (DCA), which is a simple statistical method that
20 gives a robust estimate of worst-case for a given linear metric of impact, and which has various advantages relative
21 to alternative definitions of worst-case. We present new mathematical results that clarify the interpretation of
22 DCA and we illustrate DCA with an extensive set of synthetic examples. We then apply the mean and worst-case
23 method based on DCA to EURO-CORDEX projections of future precipitation in Europe, with two different
24 impact metrics. We conclude that the mean and worst-case method based on DCA is suitable for climate projection
25 users who wish to explore the implications of the uncertainty around the ensemble mean without having to
26 calculate the impacts of every ensemble member.

27 **Keywords:** climate projection, ensemble mean, worst-case, DCA, EURO-CORDEX, precipitation

28 **Declarations**

29 **Funding**

30 G. Messori was partly supported by the Swedish Research Council Vetenskapsrådet (grant no. 2016-03724).

31 **Conflicts of Interest**

32 MS works for RMS Ltd, a private company involved in weather and climate risk modelling.

33 **Data Availability Statement**

34 The EURO-CORDEX data used in this study is freely available. Details are given at <https://euro-cordex.net>.

35 **Code availability**

36 Not applicable.

37 **Author's Contributions**

38 Stephen Jewson designed the study and the algorithms, wrote and ran the analysis code, produced the graphics
39 and wrote the text. Gabriele Messori reviewed the study in detail, Giuliana Barbato, Paola Mercogliano and
40 Jaroslav Mysiak extracted the EURO-CORDEX data and Maximiliano Sassi wrote the code to read the EURO-
41 CORDEX data. All the authors contributed to proof-reading.

42 **Acknowledgements**

43 The authors would like to thank Francesco Repola from CMCC for assisting with data extraction, and Casper
44 Christophersen, Marie Scholer and Luisa Mazzotta from EIOPA for arranging for the EURO-CORDEX data to
45 be made available.

46 **1. Introduction**

47 There is an extensive literature on how users of climate information might process ensemble climate projections,
48 including methods for bias correction (Maraun, 2016; Knutti, et al., 2017; Chen, et al., 2019), methods for
49 identifying the forced response (Barnes, et al., 2019; Sippel, et al., 2019; Wills, et al., 2020), analysis of the
50 potential benefits of spatial smoothing (Raisanen & Ylhaisi, 2010; Masson & Knutti, 2011), methods for assigning
51 weights to the different models in an ensemble (Knutti, et al., 2017; Sanderson, et al., 2017; Abramowitz, et al.,
52 2019), methods for understanding uncertainty (Deser, et al., 2010; Hawkins & Sutton, 2009; Frankcombe, et al.,
53 2015; Thompson, et al., 2015), methods for reducing uncertainty using emerging constraints (Hall, et al., 2019)
54 and methods for creating smaller and hence more manageable ensembles (Evans, et al., 2013; Herger, et al., 2018).

55 In this article, we will revisit the question of how to create smaller and more manageable ensembles. We imagine
56 a hypothetical user of climate projections who currently considers only the ensemble mean from a climate
57 projection ensemble such as the CMIP5 project (Taylor, et al., 2012), the CMIP6 project (Eyring, et al., 2016) or
58 the EURO-CORDEX project (Jacob, et al., 2014; Jacob, et al., 2020). They use an impact model which already
59 incorporates simulations of weather variability, and the reason for using climate models is to understand possible
60 changes in statistics of weather variability under climate change. They look at impacts of the ensemble mean for
61 multiple cases based on the four main RCPs (Moss, et al., 2010) or the five SSPs (Riahi, et al., 2017), for different
62 points in time and for different adaptation strategies. Their impact models are costly to run, and this is already a
63 lot of calculations. They would like to consider the impact of uncertainty around the ensemble mean, but running
64 every ensemble member for every case is not feasible. Is there, nevertheless, a way that they could take into
65 account uncertainty within each ensemble?

66 As an example, this problem often arises when including the effects of climate change in insurance industry risk
67 models for severe weather risks. These models, known as catastrophe models (Grossi & Kunreuther, 2005;
68 Mitchell-Wallace, et al., 2017), simulate present-day weather risks using their own ensembles consisting of many
69 tens of thousands of members, each of one year in length (a methodology developed in the 1960s by Don Friedman
70 (Friedman, 1972)). The models can be adjusted to incorporate aspects of climate variability and change from
71 climate models (Sassi, et al., 2019; Jewson, et al., 2019), but the catastrophe models are computationally intensive,
72 because of the large size of their ensembles and their high spatial resolution, and running them many times to
73 understand the impacts of every climate model ensemble member may not be possible for all users.

74 To bridge the gap between the two extremes of analyzing only the ensemble mean and analyzing every ensemble
75 member, one might consider using only a subset of the members of the full ensemble, either chosen randomly, or
76 according to some kind of algorithm (Evans, et al., 2013; Herger, et al., 2018). The smallest subset, apart from
77 using just the ensemble mean, would be to use the ensemble mean and one additional pattern, so that the full
78 impact model only has to be run twice. This approach has recently been studied by Scher, et al. (2021) (henceforth
79 SJM) in the context of medium range ensemble forecasts of temperature. To determine which single additional
80 pattern to use, SJM considered a linear function that gives a measure of which ensemble members are most
81 important in terms of impact. They then compared four different methods that could be used to find a single
82 reasonable worst-case deviation from the ensemble mean, given the linear impact function. 'Reasonable worst' in
83 the phrase reasonable worst-case means that the probability of this pattern should not be too low, so that the pattern
84 is realistic, and that the pattern should have a large positive value of the linear impact function relative to the
85 members of the ensemble. Two of the four methods that SJM compared were based on Directional Component
86 Analysis (DCA, Jewson (2020)), a third method consisted of taking the worst single member from the ensemble
87 and a fourth method consisted of averaging the worst 10% of the members of the ensemble. They compared these
88 four methods and found the two DCA methods to be the most robust.

89 We will expand on the ideas in Jewson (2020) and SJM and explore further the idea of defining a reasonable
90 worst-case pattern from an ensemble using DCA. DCA is a method for deriving extreme patterns from space-time
91 datasets such that the patterns have both a large linear impact and a high likelihood (where we use likelihood
92 synonymously with probability density). We extend the previous work in four ways. First, we provide additional
93 illustrative examples of how DCA identifies a worst-case pattern. For these examples we imagine applying DCA
94 to climate projections of precipitation and include examples in which the definition of linear impact is based on
95 increased precipitation in all regions, and other examples in which it is based on increased precipitation in some
96 regions, and decreased precipitation in others. This latter case is motivated by the situation in Europe where parts

97 of northern Europe are projected to experience an increase in precipitation because of climate change, while parts
98 of southern Europe are projected to experience a decrease in precipitation (European Environment Agency, 2017).
99 In this situation, a Europe-wide worst-case might consist of greater than the ensemble mean precipitation in
100 northern Europe and less than the ensemble mean precipitation in southern Europe. Second, we present various
101 additional mathematical properties of DCA that were not described in Jewson (2020) or SJM, that help to clarify
102 the interpretation of DCA. Third, we discuss in detail how the linear impact function used in DCA can be
103 considered as a linearisation of a non-linear impact function, and how the method can be generalized to quadratic
104 and cubic approximations. Fourth, we apply DCA to high-resolution multi-model climate projections from
105 EURO-CORDEX for two different linear impact functions.

106 In Sect. 2 we describe the data we will use and review the DCA methodology. In Sect. 3 we present new
107 illustrations of DCA. In Sect. 4 we present new mathematical properties of DCA that help clarify the
108 interpretation. We also discuss how to generalize DCA to quadratic and cubic impact functions. In Sect. 5 we
109 illustrate the DCA methodology with results from the EURO-CORDEX climate model ensemble. In Sect. 6 we
110 draw some conclusions. Appendices A to E include a number of related mathematical derivations.

111 **2. Data and Methods**

112

113 **2.1 Synthetic Data**

114 In section 3 we analyse synthetic ensemble data to illustrate the DCA method in various ways, and compare it
115 with using just the worst member to define the worst case. The synthetic data was created by simulating from a
116 bivariate normal distribution. The two dimensions are intended to represent changes in future annual mean
117 precipitation values at two different but nearby locations and each ensemble member is intended to represent
118 output from a different climate model. We simulate ensembles of both 10 and 1000 members, and we also simulate
119 500 repeats of the 10 member ensemble to understand the robustness of the results to the statistical sampling
120 involved in creating the ensembles. 1000 is larger than the number of climate models in existence, but using 1000
121 member ensembles is helpful for illustrating how DCA works.

122 **2.2 EURO-CORDEX data**

123 The climate model data we use in Sect. 5 is annual mean precipitation data extracted from the EURO-CORDEX
124 ensemble projections of future climate (Jacob, et al., 2014; Benestad, et al., 2017; Jacob, et al., 2020). We use data
125 from 10 separate projections, simulated by 10 different combinations of global models and regional models: a list
126 of the models used is given in Table 1. The model output is at 0.11-degree resolution (roughly 12km). Our analysis
127 is based on the ensemble member by ensemble member difference between RCP4.5 annual mean precipitation in
128 the period 2011-2040 and the baseline period 1981-2010, which we refer to as precipitation changes.

129 **2.3 DCA Definition**

130 We now give a definition and brief overview of DCA, based on Jewson (2020) and SJM. For the ensembles we
131 are considering in this article, we define DCA as follows. The ensemble members, which are spatial patterns, are
132 converted to anomalies from the ensemble mean and written as vectors, x with M components corresponding to
133 the number of spatial points. Given an ensemble of N members we write the N vectors in a matrix X . This matrix
134 has dimensions M by N . The spatial covariance matrix of the vectors, which gives the covariance between every
135 possible pair of spatial points, is given by $C = XX^T/N$, which is an M by M matrix. The total scalar impact a of
136 a spatial pattern is defined as the sum of the impact of the ensemble mean a_0 and the deviation a' of the impact
137 from a_0 due to the vector anomaly x , giving $a = a_0 + a'(x)$. We assume that the deviation $a'(x)$ is a linear
138 function of x , and we will call it the linear impact. It can be written as a weighted sum of values in the anomaly
139 pattern x as $a' = x^T r$, where the vector r gives the weights at each location. The vector r can, equivalently, be
140 interpreted as the direction of the gradient of the impact, pointing towards values of highest impact. A simple
141 example of impact that can be expressed using $a = a_0 + x^T r$ is the total precipitation change (change relative to
142 the previous climate) across a precipitation field: if x is the spatial field of precipitation anomalies, a_0 is the total
143 precipitation change of the ensemble mean and r is a vector of ones, then a is the total precipitation change due
144 to the ensemble mean plus the anomaly pattern x . A more complex example might involve using the components
145 of the vector r to apply weighting as a function of spatial variation in population density.

146 Given the above definitions the DCA pattern g is then a vector with M components given by the proportional
147 relationship:

$$148 \quad g \propto Cr \tag{1}$$

149 The DCA vector g can be interpreted as a spatial pattern. Since $C = XX^T/N$ this gives $g \propto (XX^T/N)r =$
150 $X(X^T r)/N$, which can also be written as

$$151 \quad g \propto Xw \tag{2}$$

152 where $w = X^T r$ is a vector that gives the linear impacts of the individual members of the ensemble. Based on
153 these expressions we see that the DCA pattern g can be calculated either using the covariance matrix ($g \propto Cr$)
154 or by calculating the linear-impact-weighted average of the ensemble members ($g \propto Xw$).

155 Equations (1) and (2) are proportional relationships and define the direction of the DCA vector g (i.e., the shape
156 of the spatial pattern described by g), but not the magnitude of the vector (i.e., not the amplitude of the spatial
157 pattern described by g). To make the definition of DCA unique, Jewson (2020) defines the first DCA pattern as a
158 unit vector. The length of the unit vector DCA pattern can then be scaled to an appropriate value, depending on
159 the application. Subsequent DCA patterns can also be derived, to create a set of orthogonal spatial patterns and a
160 corresponding method for matrix factorisation, although in this study we will only consider the first pattern, which
161 we will refer to simply as the DCA pattern or DCA vector.

162 **2.3.1 Mathematical Properties**

163 The mathematical properties of DCA depend on the statistical distribution of the ensemble. Jewson (2020) shows
164 that if the ensemble is distributed as a MultiVariate Normal distribution (MVN), then DCA is the anomaly spatial
165 pattern that maximises the probability density for a given value of the linear impact function (*property 1*). Part of
166 the utility of DCA arises from the fact the direction of the DCA vector is then independent of the level of linear
167 impact used in this definition, and depends only on the direction of the gradient of linear impact. Conversely, the
168 DCA pattern is also the anomaly spatial pattern that maximises the linear impact for a given value of the
169 probability density (*property 2*). These are the properties that justify the use of the DCA pattern as a pattern that
170 is representative of extremes, where extreme is defined in terms of the linear impact function.

171 If the ensemble is not MVN, but is still elliptically distributed (for example, is distributed as a multivariate t
172 distribution) then these properties may still hold: more precise details are given in Appendix A.

173 If the ensemble is not elliptically distributed it is useful to distinguish between what we will call *smoothable* and
174 *non-smoothable* ensembles. Smoothable ensembles are those that have the property that weighted linear
175 combinations of events in the ensemble are plausible alternative members of the ensemble, while non-smoothable
176 ensembles are those which do not have this property. As examples of smoothable and unsmoothable ensembles:
177 climate projections of temperature might be considered smoothable, while short-term weather forecasts of
178 localised convective precipitation would probably not be, because averaging together convective events in
179 different locations does not create a realistic field of convective events. For ensembles that are not elliptically
180 distributed but are smoothable, DCA can be considered as a reasonable non-parametric method for creating
181 extreme scenarios, based on Eq. (2) (which defines DCA as a weighted average of each ensemble member), but
182 no longer possesses optimality properties related to impact and likelihood. For ensembles that are non-smoothable
183 DCA could be calculated, but the resulting patterns are unlikely to be useful. The question of whether an ensemble
184 is smoothable or not also affects the interpretation of the ensemble mean, and in general, if it is reasonable to
185 consider using the ensemble mean as a plausible spatial pattern, then it is most likely reasonable to consider using
186 DCA. This is because both DCA and calculating the ensemble mean involve weighted linear combinations of
187 events in the ensemble (where for DCA the weights are given by Eq. (2) and for the ensemble mean the weights
188 are equal).

189 **2.3.2 Scaling**

190 In several of the examples in this article we will set the length of the DCA vector to give a reasonable
191 representation of the amplitude of the variability of the linear impact represented in the ensemble, as follows.
192 First, we determine the DCA direction g using Eq. (1) above and normalize g to be a unit vector. Second, we
193 project all the members of the ensemble onto the unit vector g to create a series of projected values. Third, we

194 calculate the standard deviation of this series of projections and set the length of the DCA vector to a value of two
195 standard deviations. This gives a pattern which is two standard deviations of ensemble variability away from the
196 ensemble mean in the direction of the DCA pattern, and hence represents a reasonable level of extreme linear
197 impact relative to the ensemble members. Within this method for scaling, the choice of two standard deviations
198 is arbitrary, and could be replaced by any other number of standard deviations, or percentiles of the distribution
199 of the projected values.

200 If the ensemble mean and the DCA pattern are used as inputs for a complex impact model, the output from the
201 complex impact model when forced with the DCA pattern scaled in this way can be used as an approximation to
202 two standard deviations of the distribution of impact as would be calculated using the brute-force and
203 computationally intensive approach of running the complex impact model on each ensemble member. In this way
204 DCA reduces the number of evaluations of the complex model from N to 2. Whether the approximation to the
205 results of the complex model is a good one depends on whether the linear impact model is a good approximation
206 to the complex impact model over the range of variability of the ensemble.

207 **2.3.3 Generalisations to Non-linear Impact Functions**

208 DCA uses a linear impact function. Real-world impact is likely, in most cases, to be non-linear, at least to some
209 degree. The linear definition of impact used in DCA is the simplest possible formulation that allows us to explore
210 the connections between the impact of a pattern and its likelihood, and to determine from that a straightforward
211 methodology for defining reasonable worst-case patterns. Within the context of reducing an ensemble to just the
212 mean and the reasonable worst case, using a linear impact function may be an appropriate level of complexity for
213 many applications, given the other uncertainties inherent in the ensemble, the approach and the impact models,
214 and given that the linear approximation only has to be a good approximation within the range of the ensemble.
215 Alternatively, the impact function can be extended to include quadratic and cubic terms, as described in Sect. 4.2
216 below. If a cubic approximation is not sufficient then it may be necessary to run the full impact model with every
217 member of the ensemble separately.

218 **3 Illustrations and Examples**

219 We now show a number of illustrations and examples of DCA applied to ensembles, extending on the illustrations
220 and examples in Jewson (2020) and SJM. We will assume the ensemble is MVN.

221 **3.1 Illustrations**

222 Figure 1 illustrates DCA in four different situations, in two dimensions. We will assume that the two dimensions
223 represent changes in annual mean precipitation at two locations. In each case the ensemble is represented by a
224 single elliptical contour of constant probability density, with higher densities inside the ellipse. The ensemble
225 mean is shown by the red dot at the centre of the ellipse. Fig. 1a illustrates a situation in which the impact is simply
226 the sum of the precipitation changes at the two locations, and so the impact vector r (illustrated by the black
227 arrow) points towards the top right corner of the diagram where the total precipitation change is greatest. A line
228 of constant impact, which is perpendicular to the impact vector r , is shown by the straight diagonal line. The DCA
229 pattern is shown by the blue dot at the point at which the straight-line is tangent to the ellipse. The DCA pattern
230 is scaled to lie on the contour of probability density shown. The DCA pattern does not align with the impact vector
231 because it also takes account of the covariance structure of the ensemble, i.e., the elliptical shape of the
232 distribution. This diagram relates to the two properties of DCA given in section 2.3.1 above as follows.
233 Considering property 1: we can see that of all points on the straight line, which have the same impact (in this case,
234 the same total precipitation change), the point that touches the ellipse is the point with the highest probability
235 density (since all the other points on the straight line lie outside the ellipse and are hence at lower probability
236 densities). Considering property 2: we can see that of all the points on the ellipse, which are the same probability
237 density, the point at which the straight line touches the ellipse is the point with highest impact (since it is the point
238 which is furthest from the ensemble mean in the direction of the impact vector). Furthermore, we can see that if
239 we move away from the DCA pattern in any direction then either the impact or the probability density will reduce:
240 moving into the ellipse or along the ellipse reduces impact, while moving out of the ellipse reduces probability
241 density.

242 Figure 1b illustrates the same ensemble (i.e., the same ellipse) as Fig. 1a but a situation in which the definition of
243 impact puts twice as much weight on precipitation change at the second location (the vertical axis) as on the
244 precipitation change at the first location (the horizontal axis). As a result, r now points more vertically than in

245 Fig. 1a, and the line of constant impact is more horizontal. This changes the DCA vector, which now has more
246 precipitation at location 2 than location 1. Fig. 1c illustrates a different ensemble, but for the same impact vector
247 as in Fig. 1a. This also changes the DCA vector relative to Fig. 1a. Finally, Fig. 1d illustrates a more complex
248 situation using a different ensemble in which the impact increases as precipitation changes increase at location 2
249 but impact *decreases* as precipitation changes increase at location 1. This would occur in the situation discussed
250 in the introduction in which at location 2 the main concern with respect to climate change and future precipitation
251 is related to increases in precipitation (e.g., such as concerns about increased flooding in the UK) while at location
252 1 the main concern is with respect to decreases in precipitation (e.g., such as concerns about increased drought in
253 some parts of Southern Europe). In this case the vector r points to the top left corner of the diagram, and the lines
254 of constant impact are correspondingly different, and run from the lower left to the upper right. The DCA direction
255 is also correspondingly very different, and selects a pattern that consists of increased precipitation at location 1
256 and decreased precipitation at location 2, relative to the ensemble mean, as the reasonable worst-case.

257 3.2 Examples

258 We now give some examples of DCA patterns calculated using synthetic ensemble data (Sect. 2.1). Our first set
259 of examples are based on synthetic ensembles with 1000 members and are shown in Fig. 2. These examples
260 correspond to the diagrams shown in Fig. 1. Figure 2a shows one ensemble with 1000 ensemble members
261 (generated using a correlation of -0.4), the ensemble mean (red dot), the direction of the impact vector r (black
262 arrow), which puts equal weight on both precipitation variables (following Fig. 1a) and the DCA pattern scaled
263 to two standard deviations of impact, as described in Sect. 2.3.2 (blue dot). The DCA pattern is calculated using
264 Eq. (1). Figure 2b shows the same ensemble, with the same ensemble members, but now with a different impact
265 vector r which puts twice as much weight on the precipitation change on the vertical axis (following Fig. 1b).
266 This shifts the DCA pattern. Figure 2c shows a different ensemble (now generated using a correlation of zero but
267 unequal variances in the two directions), but with the same impact vector as Fig. 2a (following Fig. 1c). This leads
268 to a different DCA pattern relative to Fig. 2a. Figure 2d shows a different ensemble again (generated using a
269 correlation of -0.4), and an impact vector which puts equal weight on negative precipitation change on the
270 horizontal axis and positive precipitation change on the vertical axis (following Fig. 1d). This leads to a DCA
271 pattern which also has negative precipitation change on the horizontal axis and positive precipitation change on
272 the vertical axis.

273 Overall, the illustrations in Sect. 3.1 above and these examples illustrate the way in which the DCA pattern is
274 determined by both the impact function and the shape of the probability density function of the ensemble.

275 Our second set of examples, shown in Fig. 3, are similar, but are based on only 10 ensemble members, since our
276 EURO-CORDEX ensemble only has 10 members. These ensembles were generated using a correlation of -0.4,
277 and the elliptical structure of the ensemble is now much less clear from so few members.

278 Figure 4 explores the robustness of DCA for ensembles of size 10. It shows results from creating 500 ensembles,
279 each of size 10, from the same underlying mean, variances and correlation as were used in Fig. 3. For each of the
280 500 ensembles, we identify the worst ensemble member (i.e., the one with the largest impact), and the DCA
281 pattern, and these are illustrated in the figure. The mean of the 500 ensemble means is given by the red dots, and
282 the individual ensemble members are not shown. The worst ensemble member shows large variability (Fig. 4a),
283 while the DCA pattern shows much lower variability (Fig. 4b). This shows that the DCA pattern is a more robust
284 estimate of a worst-case than the worst member of the ensemble, which is because the DCA pattern is based on
285 more information: from Eq. (1) and Eq. (2) we see that it uses information from the entire ensemble, rather than
286 from just one member. SJM studied the robustness of DCA in detail, comparing with the robustness of the worst
287 ensemble member and the average of the worst 5 ensemble members, for a 50 member ensemble of ECMWF
288 medium range temperature forecasts. They considered statistical robustness, i.e., robustness to the random
289 sampling that occurs in the creation of the ensemble, robustness to small changes in the physical domain and
290 robustness to the use of normal distributions. In all tests they found that DCA was more robust than the two
291 alternative methods they considered.

292 4 Additional Mathematical Properties and Generalisations of DCA

293 In Sect. 4.1 below we present a number of additional mathematical properties of DCA for the MVN case, that we
294 believe help with the interpretation. The idea that one pattern has multiple mathematical properties is a familiar
295 one, since the ensemble mean itself has multiple mathematical properties, each of which helps with the

296 interpretation of the ensemble mean in different ways and in different situations (for example, the ensemble mean
 297 is the pattern that minimizes the in-sample mean squared error across the ensemble, and if the ensemble is
 298 symmetrically distributed then the ensemble mean is also the ensemble median). In Sect. 4.2. below we then
 299 discuss how DCA can be generalized to non-linear impact functions.

300 **4.1 Additional Mathematical Properties of DCA**

301 The optimality properties of DCA discussed in Sect. 2.3.1 above (property 1 and property 2) are of the form “the
 302 DCA vector maximises X given Y”. In Sect. 4.1.1-4.1.2 below we will show that DCA also satisfies two
 303 statements of the simpler form “the DCA vector maximises Z”.

304 Equation (2) above shows that the DCA pattern can be considered as the linear-impact-weighted average of the
 305 members of the ensemble, which suggests that DCA may have properties related to the expectation over all
 306 possible patterns in the MVN. In Sect. 4.1.3-4.1.4 below we explore this idea and present two ways in which the
 307 DCA pattern can be considered as an expectation.

308 We will illustrate these additional properties in Fig. 5 with a simple two-dimensional example. Fig. 5a shows
 309 values of the probability density p for a bivariate normal distribution with mean zero and a correlation of -0.4,
 310 representing the probability densities for an ensemble. Darker shading indicates higher probability density, and
 311 the black arrow (in this and subsequent panels in Fig. 5) shows the direction of the impact vector r , which is in
 312 the direction (1,1). The probability density has an elliptical shape, and the green arrow shows the principle axis
 313 of the ellipse, which is also the first eigenvector of the covariance matrix. The arrow is scaled to a length equal to
 314 the square root of the corresponding eigenvalue.

315 Figure 5a can also be interpreted as showing a quantity known as the Mahalanobis distance, defined by $m =$
 316 $\sqrt{x^T C^{-1} x}$. Mahalanobis distance is a multivariate generalisation of the univariate concept of the number of
 317 standard deviations from the mean. For the MVN the Mahalanobis distance is proportional to minus the log of the
 318 probability density, and so (since numeric values are not specified for the colour scale) Fig. 5a can also be
 319 interpreted as showing the Mahalanobis distance, with *lighter* shading showing a greater distance. Fig. 5b shows
 320 values of the linear impact function, which is $a' = 30(x_1 + x_2)$, where x_1 and x_2 are the distance in the horizontal
 321 and vertical directions. The diagonal lines show constant values of this linear impact function. Fig. 5c, and all
 322 subsequent panels of Fig. 5, show the DCA pattern, given by a black cross, calculated by scaling r to be a unit
 323 vector and then using Eq. (1). Figure 5d shows the DCA pattern, given by a red circle, calculated using Eq. (2),
 324 without further scaling. The red circle in Fig. 5d represents the same spatial pattern as shown by the black cross
 325 in Fig. 5c (i.e., has the same direction from the origin) but with a slightly different length scaling.

326 **4.1.1 The DCA Pattern Maximises the Ratio of Linear Impact to Mahalanobis Distance**

327 The first new property we describe is that the DCA vector maximises the ratio of the linear impact a' to the
 328 Mahalanobis distance. We write this ratio as

$$329 \quad c(x) = \frac{a'(x)}{m(x)} \quad (3)$$

330 This property of DCA emphasizes that in the MVN case DCA finds patterns that have both a high linear impact
 331 (a large value of a') and at the same time have a high probability density, which corresponds to a low value of m .
 332 The proof that maximising Eq. (3) leads to the same expression for the DCA pattern as Eq. (1) above is given in
 333 Appendix B.

334 The ratio can also be written using the fact that $m^2 = \ln(p_0) - \ln(p)$, where p is the probability density of x and
 335 p_0 is the probability density for the ensemble mean, giving $c = a' / \sqrt{\ln(p_0) - \ln(p)}$. This expression also
 336 illustrates that DCA captures the idea of finding directions with large values of both a' and p .

337 Figure 5e shows values of the ratio $c = a'/m$, with darker shading showing larger values. We can see that there
 338 is a direction along which this ratio has the largest values which aligns with the direction of the DCA pattern given
 339 by the black cross.

340 **4.1.2 The DCA Pattern Maximises the Product of Linear Impact and Weighted Probability Density**

341 The second new property we describe is that any DCA pattern, of any length scaling, can be described as the
342 pattern that maximises the product of the linear impact a' and the probability density p to some positive power,
343 i.e., the function

$$344 \quad f(x) = p(x)^n a'(x) \quad (4)$$

345 In Appendix C we show that maximising Eq. (4) leads to a pattern which is a scaling of the DCA pattern given
346 by Eq. (1), and that different values of n give all possible scalings.

347 This property of DCA emphasizes more clearly than any of the other properties that for the MVN DCA finds
348 patterns that have both a high linear impact, and a high probability density. One could also attempt to find patterns
349 that maximise this function for probability distributions other than the MVN, although the solutions may not be
350 DCA patterns, according to the definition of DCA given in Sect. 2.3.1 above.

351 Figure 5f shows values of $f(x)$ for $n = 1$, with darker shading showing higher values. We see that there is indeed
352 a maximum in the direction of the DCA vector.

353 **4.1.3 The DCA Vector is Parallel to the Tail Conditional Expectation**

354 The third new property we describe is that, for the MVN, the direction of the DCA vector is the same as the
355 direction of the vector defined as the expectation over all possible vectors, conditional on exceeding a certain
356 value for the linear impact. We call this the tail conditional expectation. In Fig. 5b, this expectation is the
357 expectation over the region above and to the right of one of the diagonal lines. In this sense DCA can be considered
358 as a generalisation of the ensemble mean, since the tail conditional expectation gives the ensemble mean if we
359 consider exceeding impacts of minus infinity.

360 This property is shown in Appendix D below.

361 Given this property one could estimate DCA as the ensemble mean, conditional on exceeding a certain threshold
362 value for the linear impact, although this is unlikely to be a good estimator for large values of the threshold as it
363 will only use a small amount of information from the ensemble. Fig. 5g shows patterns estimated in this way, for
364 three different levels of linear impact, given by the three diagonal lines, which have impacts of -30, 0 and 30. We
365 see that the patterns do indeed lie along the DCA direction, given by the black cross.

366 This property helps explain why SJM found that using the mean of the 5 worst members of the ensemble as a
367 definition of reasonable worst case gave similar results to DCA: the mean of the 5 worst members is in fact an
368 alternative (although less precise) estimator for DCA.

369 **4.1.4 The DCA Vector is Parallel to the Weighted Tail Conditional Expectation**

370 The fourth new property we describe is that, for MVN data, the direction of the DCA vector is the same as the
371 direction of the vector defined as the expectation over all spatial patterns, weighted by the linear impact at each
372 point, and conditional on exceeding a certain value for the linear impact. We call this the *weighted* tail conditional
373 expectation. In Fig. 5b, the weighted tail conditional expectation is the expectation over the region above and to
374 the right of one of the diagonal lines, weighted at each point by the linear impact.

375 This is shown in Appendix E below.

376 A special case of this property is that the expectation over *all* patterns, weighted by the linear impact, is parallel
377 to DCA. This is the expectation version of Eq. (2).

378 Fig. 5h shows patterns estimated in this way, for three different levels of linear impact, given by the three diagonal
379 lines, which have impacts of -30, 0 and 30. The patterns calculated as weighted tail conditional expectations do
380 indeed lie on the DCA direction given by the black cross.

381 **4.1.5 Summary of Properties**

382 Given all the above, we can summarize the key properties of DCA, as applied to MVN distributed data, as follows:

- 383 1) When scaled appropriately, the DCA pattern gives the unique spatial pattern that maximises the
384 probability density, for a given level of linear impact, for any level of linear impact.

- 385 2) When scaled appropriately, the DCA pattern gives the unique spatial pattern that maximises the linear
386 impact, for a given level of probability density, for any level of probability density.
387 3) All scalings of the DCA pattern maximise the ratio of linear impact to Mahalanobis distance. All scalings
388 give the same value for this ratio.
389 4) For any given scaling, the DCA pattern is the unique spatial pattern that maximises the linear impact
390 multiplied by a positive power of the probability density. An implication of this is that for any given
391 scaling of the DCA pattern, there is no other pattern which has both a higher probability density and a
392 higher linear impact, and that any change to a DCA pattern would lead to either the probability density
393 or the impact reducing.
394 5) When scaled appropriately, the DCA pattern is the unique spatial pattern that equals the expectation of
395 all possible patterns, conditional on exceeding a certain linear impact.
396 6) When scaled appropriately, the DCA pattern is the unique spatial pattern that equals the weighted
397 expectation of all possible patterns, conditional on exceeding a certain linear impact, and weighted by
398 the linear impact.
399 7) When scaled appropriately, the DCA pattern equals the linear impact-weighted expectation of all possible
400 patterns

401 4.2 Linearisation

402 In general, the impact of a change in climate state is likely to be a complex non-linear function. Consider, for
403 instance, the relationship between changes in precipitation and flood damage, or changes in wind-speed and wind
404 damage. We will write the nonlinear impact of the climate state x as $a = w(x)$. We make the simplifying
405 assumption that a is a scalar, such as the total flood or wind damage. Considering x as an anomaly from the
406 ensemble mean as before, we can then expand the function w around the ensemble mean climate state as:

$$407 \quad a = w(x) = w(0) + x^T \nabla w + x^T \nabla^2 w x + \dots \quad (5)$$

408 If we write $r = \nabla w$ and $M = \nabla^2 w$, and neglect higher terms, this equation becomes a quadratic equation for
409 impact:

$$410 \quad a = w(0) + x^T r + x^T M x \quad (6)$$

411 This quadratic approximation only has to be a good approximation across the range of variability in the single
412 ensemble being considered, and not across the entire range of variability of x .

413 In this expression the impact for the climate state x is made up of three parts: the impact due to the ensemble mean
414 $w(0)$, the linear impact $x^T r$, and the quadratic impact $x^T M x$. The quadratic impact can then itself be split into
415 two parts: the local impact relating to the diagonal elements of M and the non-local impact relating to the off-
416 diagonal elements of M , which contains quadratic cross-terms such as $x_1 M_{12} x$ which model the impact as
417 depending on the product of climate variables at different locations. Writing $M = M^{diag} + M^{offdiag}$, Eq. (6)
418 becomes

$$419 \quad a = w(0) + x^T r + x^T M^{diag} x + x^T M^{offdiag} x \quad (7)$$

420 The derivation for DCA in Jewson (2020) is based on maximising likelihood for a given impact, and solves a
421 Lagrangian maximisation problem for the linear impact $x^T r$ with the Lagrangian given by:

$$422 \quad c = -x^T C^{-1} x + \lambda(w(0) + x^T r - a) \quad (8)$$

423 Which has the solution $x \propto Cr$. The direction of the solution does not depend on the value of the Lagrange
424 multiplier λ . For quadratic nonlinear impact we can extend the Lagrangian to

$$425 \quad c = -x^T C^{-1} x + \lambda(w(0) + x^T r + x^T M x - a) \quad (9)$$

426 Which has the solution

$$427 \quad x \propto (I - \lambda CM)^{-1} Cr = A Cr \quad (10)$$

428 Where we have written $A = (I - \lambda CM)^{-1}$. This is still a simple expression that could be readily evaluated given
429 an ensemble, the linear impact vector r and the quadratic impact matrix M . The pattern x is no longer a weighted
430 sum of the ensemble members, but is the weighted sum $S = Xw/N$ transformed by the matrix A :

431 $x \propto ACr = AXX^T r/N = AX(X^T r)/N = AXw/N = AS$ (11)

432 The pattern x is also no longer constant in direction as a function of the Lagrange multiplier. In Eq. (10), different
 433 values of the Lagrange multiplier λ lead to solutions with different values for the probability density, lengths of
 434 the vector and directions.

435 We can simplify Eq. (10) in two stages. First, we might imagine a situation in which the quadratic impact is just
 436 the weighted sum of the impacts at each location, with no cross-terms, i.e., $M^{offdiag} = 0$. This could be
 437 appropriate for wind damage as a function of wind speed, since wind damage is generally local. It would be less
 438 appropriate for flood damage as a function of precipitation, since hydrological processes may make the
 439 relationship between precipitation and flood damage non-local. Under this first simplification the matrix M is then
 440 diagonal, $M = M^{diag}$, and represents the quadratic curvature of the impact at each location.

441 Second, we might imagine a situation in which there is no quadratic impact at all, in which case the matrix M is
 442 zero. In this case the solution reverts to the linear DCA solution.

443 A similar, although slightly more complicated, analytical solution also exists for a cubic approximation to the
 444 impact, based on the analytical method for solving vector quadratic equations.

445 **4.2.1 Quadratic Impact Example**

446 Fig. 5i shows patterns generated from Eq. (10), using a quadratic impact function. These are not DCA patterns,
 447 according to our definition, but are generalisations of DCA. These patterns correspond to the same linear impact
 448 vector as used in the previous panels, along with a quadratic impact matrix M given by the identity matrix, with
 449 values of λ of -2, 0 and 2. We see that the patterns for different values of λ are no longer parallel, as expected.

450 **5 EURO-CORDEX Results**

451 We now show DCA patterns derived from the EURO-CORDEX data described in Sect. 2.2. Figure 6a shows the
 452 ensemble mean for the EURO-CORDEX data, corresponding to precipitation changes for the time period 2011-
 453 2040, relative to the baseline 1981-2010, under RCP4.5. We see a pattern of increasing precipitation in northern
 454 Europe and decreasing precipitation in southern Europe, as has been described in previous studies and reports
 455 (European Environment Agency, 2017). Figure 6b shows the ensemble standard deviation of the changes, and
 456 Figure 6c shows the ensemble mean plus twice the standard deviation at each grid-point. Adding two standard
 457 deviations (as opposed to subtracting two standard deviations) is relevant for a situation in which the concern is
 458 excess precipitation at individual locations. The ensemble mean plus two standard deviations gives much higher
 459 values of precipitation change across the domain than the ensemble mean. Whether or not the pattern created by
 460 adding two standard deviations at every location is a reasonable pattern of uncertainty around the ensemble mean
 461 depends on the variable and the ensemble. For a sea-level ensemble, in which the different ensemble members
 462 differ only because they have a different global mean sea-level, it may be reasonable, as the different ensemble
 463 members may consist of the same pattern simply lifted up and down. For many other variables, including
 464 precipitation, in which the differences between ensemble members are likely to exhibit complex spatial variability,
 465 it would likely not be reasonable. This is because it is highly unlikely that any future realisation of climate would
 466 consist of two standard deviations from the mean at every location at the same time. As a result, the ensemble
 467 mean plus two standard deviations pattern shown here is only suitable for understanding possible precipitation
 468 risks at each location separately, but not for understanding precipitation risk over the whole domain, and the
 469 pattern does not form a useful candidate for reasonable worst-case for the domain as a whole. Figure 6d shows an
 470 alternative way to combine the ensemble mean with the standard deviation. It shows the ensemble mean plus two
 471 standard deviations in the regions where the ensemble mean is positive, and the ensemble mean minus two
 472 standard deviations in the regions where the ensemble mean is negative. This is perhaps more relevant than adding
 473 two standard deviations everywhere, and reflects the idea (as discussed in the introduction and in Sect. 3.1 above)
 474 that where the ensemble mean is positive there may be concern about increasing precipitation, and where the
 475 ensemble mean is negative there may be concern about decreasing precipitation. However, as with simply adding
 476 two standard deviations everywhere, this is also not a realistic pattern of climate uncertainty and is also not a
 477 candidate for worst-case over the whole domain.

478 Figure 7 shows the results of the DCA analysis. Figure 7a shows the DCA pattern for this ensemble, scaled to two
 479 standard deviations using the method described in Sect. 2.3.2, based on a linear impact function that puts equal
 480 weight on positive precipitation at all locations. We see positive precipitation anomalies distributed throughout

481 the domain, with larger values over the Alps and parts of South Eastern Europe. There are also some negative
482 precipitation anomalies: this indicates that there are spatial anti-correlations of precipitation within the ensemble,
483 such that the occurrence of a pattern with only positive anomalies is low probability. Unlike the local two standard
484 deviation pattern shown in Fig. 6c, this pattern, if the statistical assumptions are correct, is a realistic pattern of
485 variability that has a reasonable likelihood of occurrence given the ensemble. It has all the properties of DCA
486 discussed in Sect. 4: for this level of total precipitation anomaly, there is no other pattern with higher likelihood;
487 also, there is no pattern with higher total precipitation anomaly for the same likelihood; this pattern maximises
488 both total precipitation anomaly divided by Mahalanobis distance and total precipitation anomaly multiplied by
489 probability density to some positive power; the pattern is proportional to (i.e., the vector is parallel to) the
490 expectation over all possible patterns weighted by their linear impact, and finally there is no possible adjustment
491 to this pattern which could increase both the total precipitation anomaly and the likelihood. Figure 7c shows the
492 sum of the ensemble mean with this DCA pattern. We see that precipitation amounts have increased over much
493 of Northern Europe, relative to the ensemble mean, but to a much lesser extent than was seen in the ensemble
494 mean plus two standard deviations pattern in Fig. 6c, which emphasizes further that Fig. 6c is not a realistic
495 pattern. The ensemble mean plus the DCA pattern would be an appropriate forcing for complex flood risk models,
496 to estimate a reasonable worst-case for flood risk in Europe.

497 Figure 7b shows the DCA pattern for the EURO-CORDEX ensemble based on a linear impact function that puts
498 equal weight on positive precipitation change at locations where the ensemble mean is positive, and negative
499 precipitation change at locations where the ensemble mean is negative. This relates to the cases illustrated in Fig.
500 1d and Fig. 2d, and to the mean plus/minus two standard deviations example shown in Fig. 6c. In this case the
501 DCA pattern shows positive precipitation anomalies in much of Northern Europe, but negative anomalies in Spain
502 and Northern Italy. Figure 7d shows the sum of the ensemble mean and this DCA pattern. In combination they
503 again show increasing precipitation in Northern Europe and decreasing precipitation in Southern Europe, but to a
504 lesser extent than the pattern given by adding and subtracting two standard deviations, as shown in Fig. 6d. Based
505 on the impact function, and the variability and correlations in the climate model ensemble, the ensemble plus this
506 DCA pattern is an indication of what the reasonable worst-case for changes in European precipitation might look
507 like. This pattern would be an appropriate forcing for complex models for combined flood and drought risk, to
508 estimate a reasonable worst-case outcome in Europe.

509 **6 Conclusion**

510 Ensemble climate projections present a large amount of information and ideally, given infinite time and resources,
511 users of climate projections would consider the possible impact of every ensemble member in their analysis.
512 However, this may not always be feasible since some impact models are simply too computationally intensive to
513 run for every ensemble member, every RCP or SSP, every socio-economic scenario (such as migration scenarios),
514 every adaptation scenario (such as flood defence building scenarios), and every time point required. In these
515 situations, an alternative to considering the whole ensemble is to use a smaller ensemble, and an extreme case of
516 using a smaller ensemble is to use the ensemble mean and just one other pattern, carefully selected to be
517 representative of possible extremes of impact. We refer to this as the mean and reasonable worst-case approach
518 (Scher et al. (2021)). One way to create a single worst-case pattern is by adding (or subtracting) two standard
519 deviations locally. However, the spatial pattern that is created in this way is not, in most situations, a reasonable
520 pattern of uncertainty since it assumes unrealistically high correlations of the uncertainty between locations.
521 Another alternative would be to consider the worst member of the ensemble. However, the worst member is highly
522 affected by the randomness of the ensemble generation process, and hence is not robust. In a multi-model
523 ensemble, in which some models may be less realistic than others, there is also a risk that the model that determines
524 the worst member may be one of the less realistic models. Following Scher et al., (2021), we have investigated a
525 third option, which is to use the statistical method of DCA (Jewson (2020)).

526 We have extended the work of Jewson (2020) and Scher et al., (2021) in a number of ways. We have given
527 additional illustrations and simulated examples of DCA, including a case where the highest linear impacts are
528 defined by increasing precipitation in some locations and decreasing precipitation in others. We have presented
529 several new properties of DCA for multivariate normally distributed data, including (a) optimality properties that
530 avoid the use of Lagrangian calculus and show that DCA maximises certain simple functions related to probability
531 and linear impact and (b) properties that show that DCA can be interpreted as an expectation in several different
532 ways, including as a generalisation of the ensemble mean from the expectation over all patterns to the expectation
533 over all patterns with linear impact over a threshold. These new properties give additional insight and help with

534 interpretation. We have also discussed how the linear impact function used in DCA can be derived as an
 535 approximation to a more general non-linear impact function, and shown that a higher order quadratic
 536 approximation is possible, and is scarcely more complex to apply than DCA. A cubic approximation is also
 537 possible. Finally, we have applied DCA to a high-resolution EURO-CORDEX climate projection ensemble, and
 538 shown that it gives a reasonable worst-case that is materially less severe than adding or subtracting two standard
 539 deviations from the mean locally.

540 The properties of DCA can be summarized as follows. If we assume that the ensemble is multivariate normally
 541 distributed then DCA factors in both the probability density of different patterns, and their linear impacts, to derive
 542 a pattern that has both high probability density and high linear impact, relative to other patterns. As such it is a
 543 good candidate for a pattern that could be used as the definition of reasonable worst-case. The DCA pattern is
 544 realistic, robust and possesses a number of optimal mathematical properties. Some of the mathematical properties
 545 also hold if the ensemble is not multivariate normal distributed, but has a distribution which is one of the
 546 commonly used members of the wider class of distributions known as elliptical distributions, which includes, for
 547 example, the multivariate t distribution. If the ensemble is not elliptically distributed but the variability in the
 548 ensemble is such that averaging together patterns gives realistic alternative patterns, which we call a smoothable
 549 ensemble, then DCA is realistic and robust but loses the optimal mathematical properties. If the variability in the
 550 ensemble is such that averaging together patterns does not give realistic alternative patterns, i.e., the ensemble is
 551 not smoothable, then neither DCA, nor the ensemble mean itself, are likely to be very useful, since they are both
 552 created by averaging patterns. Unsmoothable ensembles may arise, for instance, when considering an ensemble
 553 of daily precipitation values, but are unusual when considering climate time averages.

554 Using the ensemble mean and one additional pattern does not give a full picture of the uncertainty around the
 555 ensemble mean: that can only be achieved by a deeper analysis, involving all the ensemble members. However,
 556 if there are practical reasons due to resource limitations for why it is only possible to consider the ensemble mean
 557 and one additional pattern, DCA is a strong candidate for the most useful pattern to look at.

558 **Appendix A: Mathematical Properties of DCA for Elliptical Distributions**

559 Elliptical distributions are those multivariate distributions for which the probability density for anomalies x from
 560 the mean can be written as

$$561 \quad p(x) = k f(x^T C^{-1} x) \tag{A1}$$

562 where k is a normalising constant. Examples are the multivariate normal distribution and the multivariate t
 563 distribution. If the function f is strictly decreasing (as it is for the multivariate normal and multivariate t)
 564 then maximising $p(x)$ is equivalent to minimising $x^T C^{-1} x$. The derivations of property 1 and property 2 (given in
 565 Jewson (2020)) are therefore still valid. Alternatively, we can rederive DCA from Eq. (A1) as follows.

566 In Jewson (2020) DCA is derived using the Lagrange function

$$567 \quad c = -x^T C^{-1} x + 2\lambda(x^T r - a') \tag{A2}$$

568 Using Eq. (A1) the Lagrange function becomes:

$$569 \quad c = -k f(x^T C^{-1} x) + 2\lambda(x^T r - a') \tag{A3}$$

570 which has the maximum if

$$571 \quad k f'(x^T C^{-1} x) C^{-1} x = \lambda r \tag{A4}$$

572 If f is strictly decreasing then f' is never zero, and this equation gives the same solution as Eq. (1) ($x \propto Cr$).

573 To cover all elliptical distributions, including those that are not strictly decreasing, property 1 has to be amended
 574 to become "DCA is the spatial pattern that minimises the Mahalanobis distance for a given value of the linear
 575 impact function".

576 **Appendix B: The DCA Pattern Maximises the Ratio of Linear Impact to Mahalanobis Ratio**

577 We will now show that the DCA pattern provides a solution to the question: given an ensemble with covariance
 578 matrix C , what is the spatial pattern x that maximises the ratio of the linear impact $a' = x^T r$ to the Mahalanobis

579 distance from the ensemble mean $m(x) = \sqrt{x^T C^{-1} x}$. The Mahalanobis distance represents the distance between
 580 the pattern x and the origin, measured using a metric that takes into account the covariance structure: it can be
 581 loosely described as being proportional to the number of equally-spaced contour lines of probability density
 582 between the origin and the pattern x . In one dimension it is the number of standard deviations from the mean. This
 583 derivation applies to any probability distribution, although it is most meaningful for elliptically distributed
 584 ensembles.

585 We will consider the function

$$586 \quad c(x) = \frac{a'(x)}{m(x)} = \frac{x^T r}{\sqrt{x^T C^{-1} x}} \quad (\text{B1})$$

587 The length of the vector x does not affect the ratio c because it cancels between the numerator and the
 588 denominator.

589 Differentiating Eq. (B1) by the vector x gives

$$590 \quad \frac{dc}{dx} = \left(m \frac{da'}{dx} - a' \frac{dm}{dx} \right) / m^2 = \left(mr - \frac{a' C^{-1} x}{m} \right) / m^2 = (m^2 r - a' C^{-1} x) / m^3 \quad (\text{B2})$$

591 Setting this equation to zero gives

$$592 \quad m^2 r = a' C^{-1} x \quad (\text{B3})$$

593 And hence

$$594 \quad m^2 C r = a' x \quad (\text{B4})$$

595 This is a vector equality, and the two sides of this equation must be parallel, from which we see that x must be
 596 parallel to $C r$, which means it is parallel to the DCA pattern given by Eq. (1). Since the length of the vectors on
 597 both sides of Eq. (B4) are proportional to the length of x squared, this equation says nothing about the length of
 598 x : any length of x is a solution. This is confirmed by the example shown in Fig. 5e.

599 **Appendix C: The DCA Pattern Maximises the Product of Linear Impact and Weighted Probability Density**

600 We now show that, for MVN ensembles, DCA provides a solution to the question: what pattern maximises the
 601 product of the linear impact and the weighted probability density? This property emphasizes directly that DCA
 602 finds patterns that both have a high linear impact and have a high probability density. We consider the function:

$$603 \quad f(x) = p^n(x) a'(x) \quad (\text{C1})$$

604 where n is positive. Changing the value of n varies the weight on the probability density, relative to the impact.

605 Differentiating with respect to x gives

$$606 \quad \frac{df}{dx} = \frac{d(p^n a')}{dx} = p^n \frac{da'}{dx} + n a' p^{n-1} \frac{dp}{dx} = p^n r - n x^T r p^n C^{-1} x = p^n (r - n x^T r C^{-1} x) \quad (\text{C2})$$

607 Setting this equation equal to zero gives

$$608 \quad n x^T r x = C r \quad (\text{C3})$$

609 This is a vector equality, and the two sides of this equation must be parallel, from which we see that x must be
 610 parallel to $C r$, which means it is parallel to the DCA pattern given by Eq. (1). The lengths of the vectors on both
 611 sides must also be equal which gives

$$612 \quad x = \frac{C r}{\sqrt{n r^T C r}} \quad (\text{C4})$$

613 This is the unique solution to Eq. (C1) and is a scaled version of DCA. Large values of n make the solution shorter.
 614 Every scaling of DCA is a solution of Eq. (C1) for a different value of n .

615 **Appendix D: The DCA Vector is Parallel to the Tail Conditional Expectation**

616 To derive this property, first we need to show that the DCA pattern is parallel to the impact conditional
 617 expectation, i.e., the vector derived as the expectation over all possible vectors, conditional on a certain value for
 618 the linear impact. In Fig. 5b, this expectation is the expectation along one of the diagonal lines. In greater than
 619 two dimensions, lines of constant linear impact become planes and hyperplanes, and this expectation is then the
 620 expectation over one of these planes or hyperplanes.

621 This initial property can be shown as follows. Property 1 from Sect. 2.3.1 above states that DCA maximises
 622 probability density for a given level of linear impact. For an MVN in two or more dimensions, the probability
 623 density for a given level of linear impact is also an MVN, in a space with one fewer dimension. For instance, in
 624 two dimensions the subspace defined by a given level of linear impact is a line (see the lines in Fig. 5b) and the
 625 probability density of points on this line is a univariate normal. In three dimensions the subspace defined by a
 626 given level of linear impact is a plane, and the probability density of patterns on this plane is a bivariate normal.

627 To demonstrate this, consider a two-dimensional case, with dimensions x and y , and consider a line of constant
 628 impact $x + y = \text{const}$. We can parametrize distance along this line using the value of x and so the probability
 629 density, conditional on being on this line, can be written as $p(x|x + y)$. Using Bayes' theorem we can factorize
 630 this into

$$631 \quad p(x|x + y) = \frac{p(x+y|x)p(x)}{p(x+y)} \quad (\text{D1})$$

632 The terms on the RHS are all normal distributions and combine to form a normal distribution. As a result, the
 633 LHS must also be a normal distribution.

634 This demonstration can be extended to other linear impact functions, and to multivariate distributions. It does not
 635 work analogously for the multivariate t distribution, since the distributions on the RHS of Eq. (D1) would not
 636 combine to be a multivariate t distribution.

637 The point with maximum probability density of an MVN is also the mean of that MVN (just as the mode and
 638 mean coincide for a univariate normal distribution) and so the DCA pattern is the mean of the reduced dimension
 639 MVN.

640 We write this property for a pattern x , for any value of a' , as the proportional relationship:

$$641 \quad E(x|x^T r = a') \propto Cr \quad (\text{D2})$$

642 We will integrate this expression over a range of levels of linear impact a' , and since the integral of DCA patterns
 643 is a DCA pattern, we find that DCA is also the expectation conditional on a range of linear impacts. Integrating
 644 Eq. (D2) over a range of linear impacts gives

$$645 \quad \int_u^v E(x|x^T r = a') da' \propto \int_u^v Cr da' \quad (\text{D3})$$

646 The LHS is equal to $E(x|x^T r \in (u, v))$. Since Cr does not depend on a' the RHS simplifies to Cr , giving

$$647 \quad E(x|x^T r \in (u, v)) \propto Cr \quad (\text{D4})$$

648 For instance, we could integrate over the region between two of the diagonal lines in Fig. 5b.

649 Setting $v = \infty$ gives the special case

$$650 \quad E(x|x^T r \in (u, \infty)) \propto Cr \quad (\text{D5})$$

651 in which the range extends to infinity on one side, which we refer to as 'tail conditioning', showing that DCA is
 652 the tail conditional expectation. If the range extends to infinity on both sides, then the expectation becomes the
 653 ensemble mean, which corresponds to the DCA pattern with a length of zero. In this sense the DCA pattern is a
 654 generalisation of the ensemble mean.

655 **Appendix E: The DCA Vector is Parallel to the Weighted Tail Conditional Expectation**

656 This property also follows from Eq. (D2). Since DCA is the expectation of the spatial pattern, conditional on a
 657 certain value for the linear impact, it is also the expectation of the spatial pattern weighted by the linear impact,
 658 conditional on a certain value for the linear impact. Integrating over a range of impacts then shows that DCA is

659 the expectation of the spatial pattern, weighted by the linear impact at each point, conditional on exceeding a
660 certain value for the linear impact.

661 Starting with Eq. (D2), multiplying both sides by any function of a' , $h(a')$ and integrating over a range of values
662 of a' gives:

$$663 \int_u^v h(a') E(x|x^T r = a') da' \propto \int_u^v h(a') Cr da' \quad (E1)$$

664 Considering the LHS first: writing the expectation as an integral:

$$665 LHS = \int_u^v h(a') \int_{x \in V_1} xp(x) dV_1 da' = \int_u^v \int_{x \in V_1} h(a') xp(x) dV_1 da' \quad (E2)$$

666 where V_1 is the volume defined by the values of x that satisfy $x^T r = a'$, dV_1 is a volume element in this volume,
667 and $h(a')$ can be taken inside the dV_1 integral because it is a constant within this volume.

668 The two integrals can then be combined into one, giving:

$$669 LHS = \int_{x \in V_2} h(a') xp(x) dV_2 = E(h(a')x|x \in V_2) \quad (E3)$$

670 where V_2 is the volume defined by the values of x that satisfy $x^T r \in (u, v)$, dV_2 is a volume element in this
671 volume, and $dV_2 = dV_1 da'$. Considering the RHS of Eq. (E1), and integrating in the same way

$$672 RHS = \int_u^v h(a') Cr da' = Cr \int_u^v h(a') da' \propto Cr \quad (E4)$$

673 Combining Eq. (E3) and Eq. (E4) gives:

$$674 E(h(a')x|x \in V_2) \propto Cr \quad (E5)$$

675 Setting $v = \infty$ gives the special case

$$676 E(h(a')x|x \in V_3) \propto Cr \quad (E6)$$

677 where V_3 is the volume defined by the values of x that satisfy $x^T r \in (u, \infty)$. This is what we set out to prove: the
678 weighted tail conditional expectation of over all possible patterns is parallel to DCA.

679 Setting both $u = -\infty$ and $v = \infty$ gives the special case

$$680 E(h(a')x) \propto Cr \quad (E7)$$

681 which says that the expectation over all patterns, weighted by the linear impact, is parallel to DCA. This is the
682 expectation version of Eq. (2).

683 Bibliography

684 Abramowitz, G. et al., 2019. Model dependence in multi-model climate. *Earth Syst. Dynam.*, Volume 10, pp.
685 91-105.

686 Barnes, E. et al., 2019. Viewing Forced Climate Patterns Through an AI Lens. *GRL*, 46(22), pp. 13389-13398.

687 Benestad, R. et al., 2017. *Guidance for EURO-CORDEX*. [Online]

688 Available at: [https://www.euro-cordex.net/imperia/md/content/csc/cordex/euro-cordex-guidelines-version1.0-](https://www.euro-cordex.net/imperia/md/content/csc/cordex/euro-cordex-guidelines-version1.0-2017.08.pdf)
689 [2017.08.pdf](https://www.euro-cordex.net/imperia/md/content/csc/cordex/euro-cordex-guidelines-version1.0-2017.08.pdf)

690 [Accessed 9 1 2021].

691 Chen, J. et al., 2019. Bias correcting climate model multi-member ensembles to assess climate change impacts
692 on hydrology. *Climatic Change*, 153(3), pp. 361-377.

693 Deser, C., Phillips, A., Bourdette, V. & Teng, H., 2010. Uncertainty in climate change projections: the role of
694 internal variability. *Climate Dynamics*, Volume 38, p. 527-546.

695 European Environment Agency, 2017. *Indicator Assessment: Mean Precipitation*. [Online]

696 Available at: <https://www.eea.europa.eu/data-and-maps/indicators/european-precipitation-2/assessment>
697 [Accessed 15 4 2020].

- 698 Evans, J., Ji, F., Ambramowitz, G. & Ekstrom, M., 2013. Optimally choosing small ensemble members to
699 produce robust climate simulations. *Environ. Res. Lett.*, Volume 8.
- 700 Eyring, V. et al., 2016. Overview of the Coupled Model Intercomparison Project Phase 6 (CMIP6) experimental
701 design and organization. *Geosci. Model Dev.*, Volume 9, pp. 1937-1958.
- 702 Frankcombe, L., England, M., Mann, M. & Steinman, B., 2015. Separating Internal Variability from the
703 Externally Forced Climate Response. *J. Clim.*, 28(20), p. 8184–8202.
- 704 Friedman, D., 1972. Insurance and the Natural Hazards. *ASTIN*, Volume 7, pp. 4-58.
- 705 Grossi, P. & Kunreuther, H., 2005. *Catastrophe Modelling: A new approach to managing risk*. NY: Springer.
- 706 Hall, A., Cox, P., Huntingford, C. & Klein, S., 2019. Progressing emergent constraints on future climate change.
707 *Nature climate change*, Volume 9, pp. 269-278.
- 708 Hawkins, E. & Sutton, R., 2009. The Potential to Narrow Uncertainty in Regional Climate Predictions. *BAMS*,
709 90(8), p. 1095–1108.
- 710 Hawkins, E. & Sutton, R., 2012. Time of emergence of climate signals. *GRL*, 39(1), pp. 1-6.
- 711 Herger, N. et al., 2018. Selecting a climate model subset to optimise key ensemble properties. *Earth Syst.*
712 *Dynam.*, Volume 9, pp. 135-151.
- 713 Jacob, D., Petersen, J. & authors, 2014. EURO-CORDEX: new high-resolution climate change projections for
714 European impact research. *Reg Environ Change*, Volume 14, pp. 563-578.
- 715 Jacob, D., Teichmann, C. & authors, 2020. Regional climate downscaling over Europe: perspectives from the
716 EURO-CORDEX community. *Regional Environmental Change*, Volume 20.
- 717 Jewson, S., 2020. An Alternative to PCA for Estimating Dominant Patterns of Climate Variability and
718 Extremes, with Application to U.S. and China Seasonal Rainfall. *Atmosphere*, 11(4), p. 354.
- 719 Jewson, S., Barnes, C., Cusack, S. & Bellone, E., 2019. Adjusting catastrophe model ensembles using
720 importance sampling, with application to damage estimation for varying levels of hurricane activity. *Met Apps*,
721 Volume 27, pp. 1-14.
- 722 Knutti, R. et al., 2017. A climate model projection weighting scheme accounting for performance and
723 interdependence. *GRL*, Volume 44, pp. 1909-1918.
- 724 Maraun, D., 2016. Bias Correcting Climate Change Simulations. *Curr. Clim. Change Rep.*, Volume 2, p. 211.
- 725 Masson, D. & Knutti, R., 2011. Spatial-Scale Dependence of Climate Model Performance in the CMIP3
726 Ensemble. *J. Clim.*, Volume 24, pp. 2680-2692.
- 727 Mitchell-Wallace, K., Jones, M., Hillier, J. & Foote, M., 2017. *Natural Catastrophe Risk Management and*
728 *Modelling*. s.l.:Wiley Blackwell.
- 729 Moss, R. et al., 2010. The next generation of scenarios for climate change research and assessment. *Nature*,
730 Volume 463, pp. 747-756.
- 731 Raisanen, J. & Ylhaisi, J., 2010. How Much Should Climate Model Output Be Smoothed in Space?. *J. Clim.*,
732 Volume 24, pp. 867-880.
- 733 Riahi, K. et al., 2017. The Shared Socioeconomic Pathways and their energy, land use, and greenhouse gas
734 emissions implications: An overview. *Global Environmental Change*, Volume 42, pp. 153-168.
- 735 Sanderson, B., Wehner, M. & Knutti, R., 2017. Skill and independence weighting for multi-model assessments.,
736 *Geosci. Model Dev.*, Volume 10, pp. 2379-2395.
- 737 Sassi, M. et al., 2019. Impact of climate change on European winter and summer flood losses. *Advances in*
738 *Water Resources*, Volume 129, pp. 165-177.

739 Scher, S., Jewson, S. & Messori, G., 2021. Robust worst-case scenarios from ensemble forecasts. *Wea.*
740 *Forecasting*, Volume (in press).

741 Sippel, S. et al., 2019. Uncovering the Forced Climate Response from a Single Ensemble Member Using
742 Statistical Learning. *J. Clim.* , 32(17), p. 5677–5699.

743 Stainforth, D. et al., 2005. Uncertainty in predictions of the climate response to rising levels of greenhouse
744 gases. *Nature*, 433(7024), pp. 403-406.

745 Taylor, K., Stouffer, R. & Meehl, G., 2012. An Overview of CMIP5 and the Experiment Design. *BAMS*, 93(4),
746 pp. 485-498.

747 Thompson, D. et al., 2015. Quantifying the Role of Internal Climate Variability in Future Climate Trends. *J.*
748 *Clim.*, 28(16), p. 6443–6456.

749 Wills, R. et al., 2020. Pattern Recognition Methods to Separate Forced Responses from Internal Variability in
750 Climate Model Ensembles and Observations. *J. Clim.* , 33(20), p. 8693–8719.

751 Yip, S., Ferro, C., Stephenson, D. & Hawkins, E., 2011. A Simple, Coherent Framework for Partitioning
752 Uncertainty in Climate Predictions. *J. Clim.*, 24(17), p. 4634–4643.

753

754 **Tables**

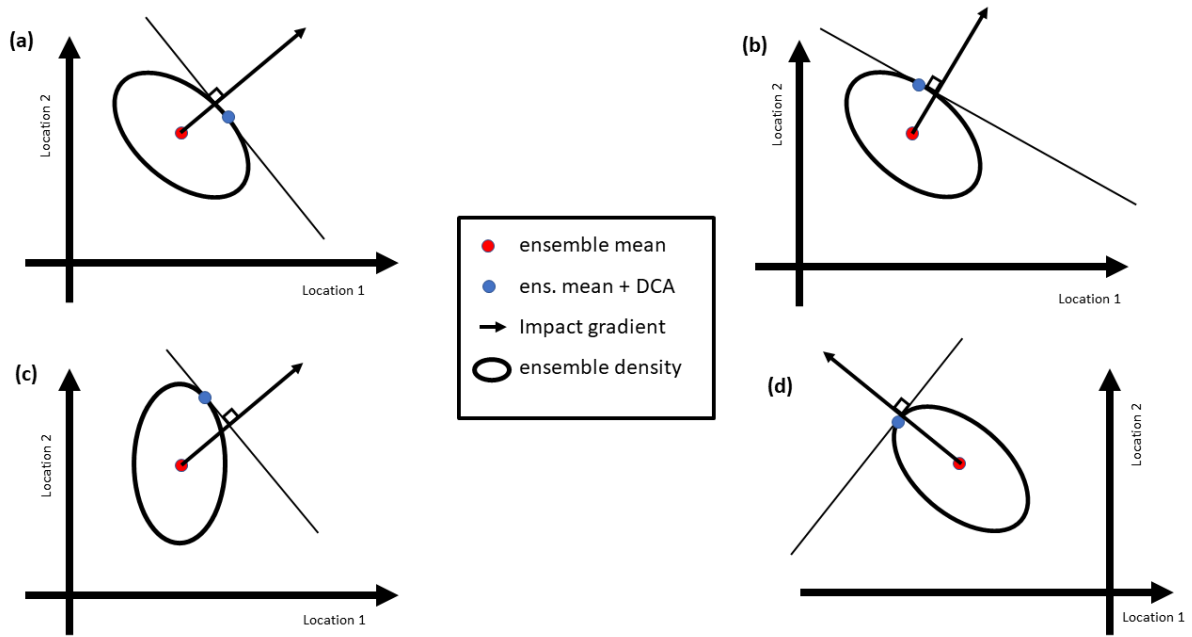
Model	Driving GCM	GCM Member	RCM
M1	CNRM-CM5	r1i1p1	ALADIN53
M2	IPSL-CM5A-MR	r1i1p1	RCA4
M3	CNRM-CM5	r1i1p1	RCA4
M4	CNRM-CM5	r1i1p1	CCLM4-8-17
M5	EC-EARTH	r12i1p1	CCLM4-8-17
M6	EC-EARTH	r12i1p1	RACMO22E
M7	EC-EARTH	r12i1p1	RCA4
M8	EC-EARTH	r1i1p1	RACMO22E
M9	EC-EARTH	r3i1p1	HIRHAM5
M10	IPSL-CM5A-MR	r1i1p1	WRF331F

755

756 Table 1: The climate models used in this study.

757 **Figures**

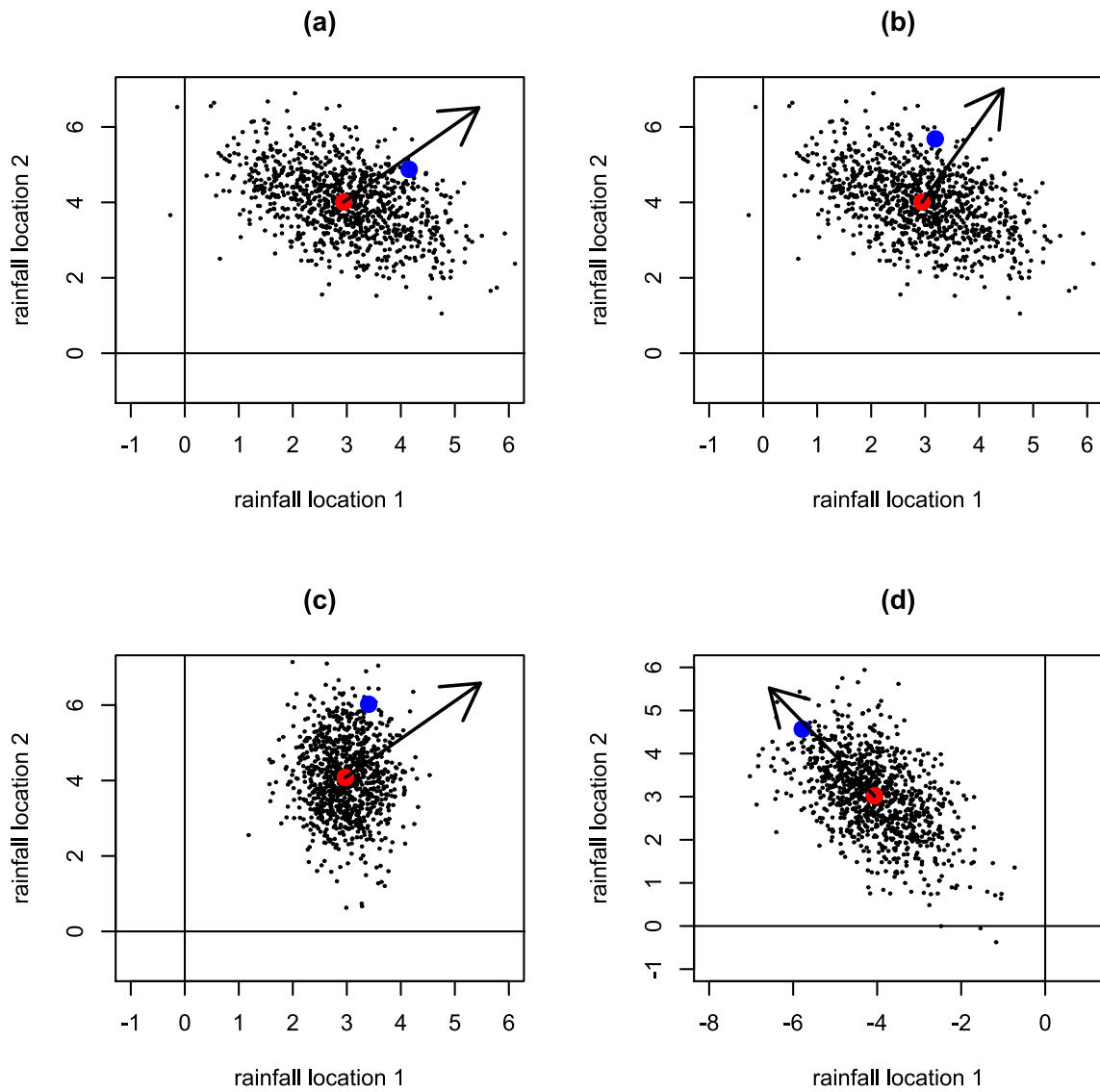
758



759

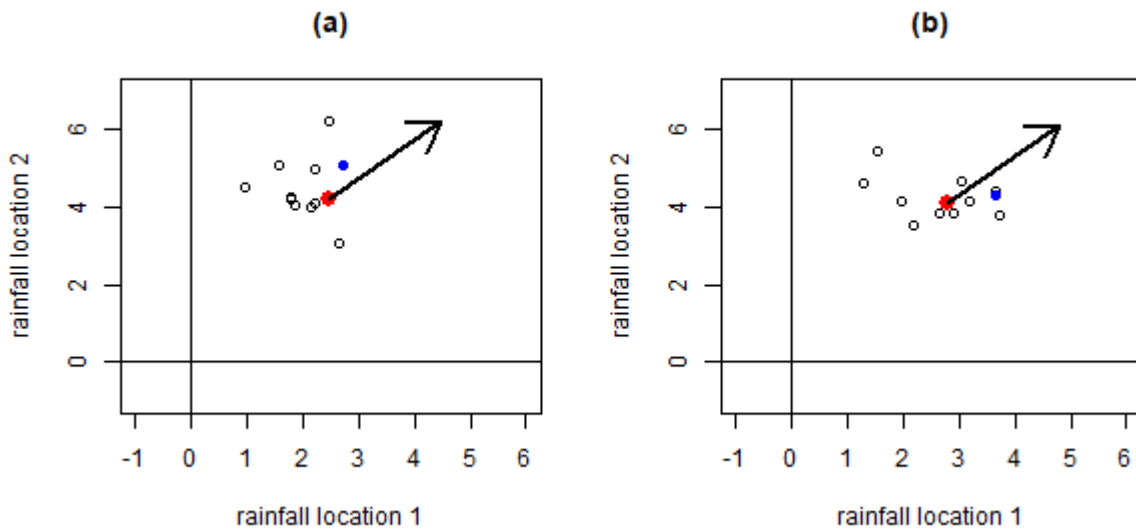
760 **Figure 1** Four illustrations of Directional Component Analysis (DCA), applied to climate variables at locations 1
 761 and locations 2. The ellipse in each case illustrates a contour of probability density for an ensemble prediction for
 762 these two locations. The ensemble is assumed to be bivariate normally distributed. The red dot in each case
 763 illustrates the ensemble mean, the arrow indicates the gradient of increasing impact, the straight line, which is
 764 perpendicular to the arrow, indicates a line of constant impact and the blue dot indicates the resulting DCA pattern.
 765 Examples (a) and (b) show the same ensemble, but different directions of impact, and hence different DCA
 766 patterns. Examples (a) and (c) show different ensembles, but the same direction of impact, and hence different
 767 DCA patterns. Example (d) shows a different ensemble and a new direction of impact

768



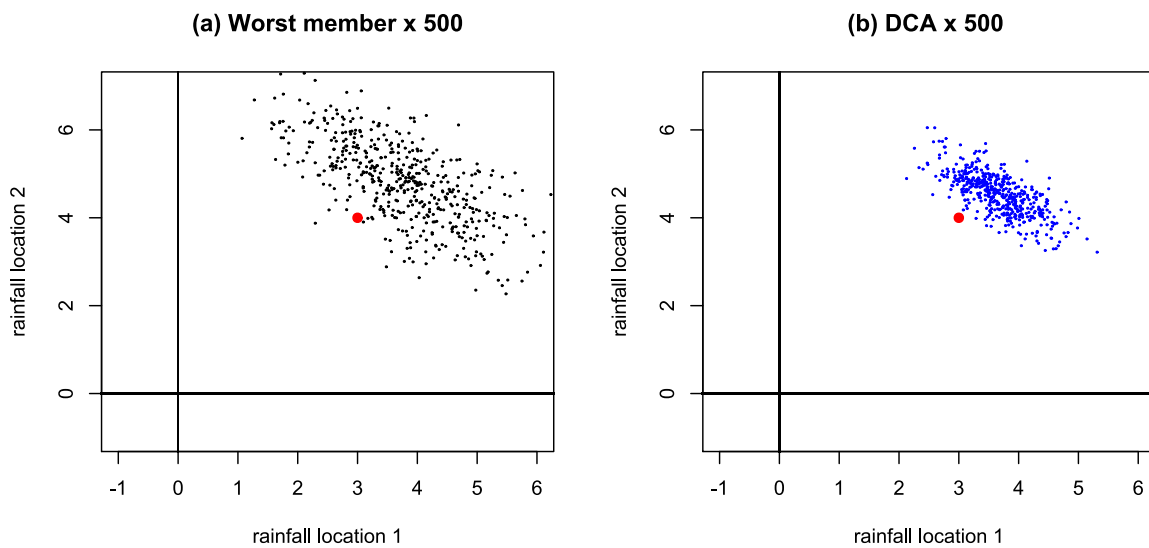
769

770 **Figure 2** Four randomly generated 1000 member examples and related quantities. In each case the ensemble
 771 members are shown by black dots, the ensemble mean is shown by a red dot, the gradient of increasing impact is
 772 shown by the arrow and the ensemble mean plus the DCA pattern, scaled to two standard deviations of impact,
 773 is shown by a blue dot. Examples (a) and (b) use the same ensemble, while examples (a) and (c) use the same impact
 774 vector. These examples correspond to the illustrations in Fig. 1



775

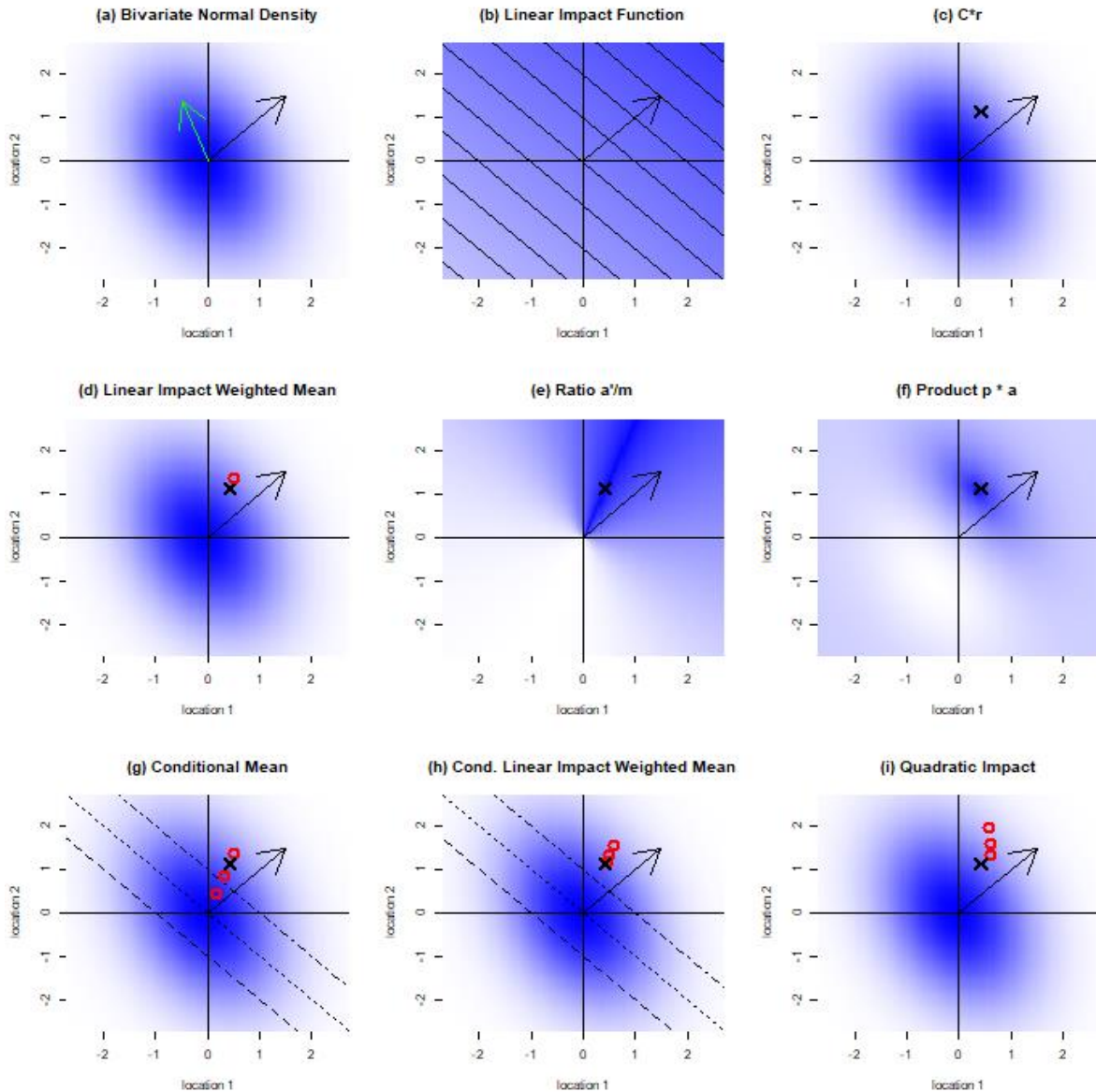
776 **Figure 3** As Fig. 2a, but now for two randomly generated 10 member ensembles



777

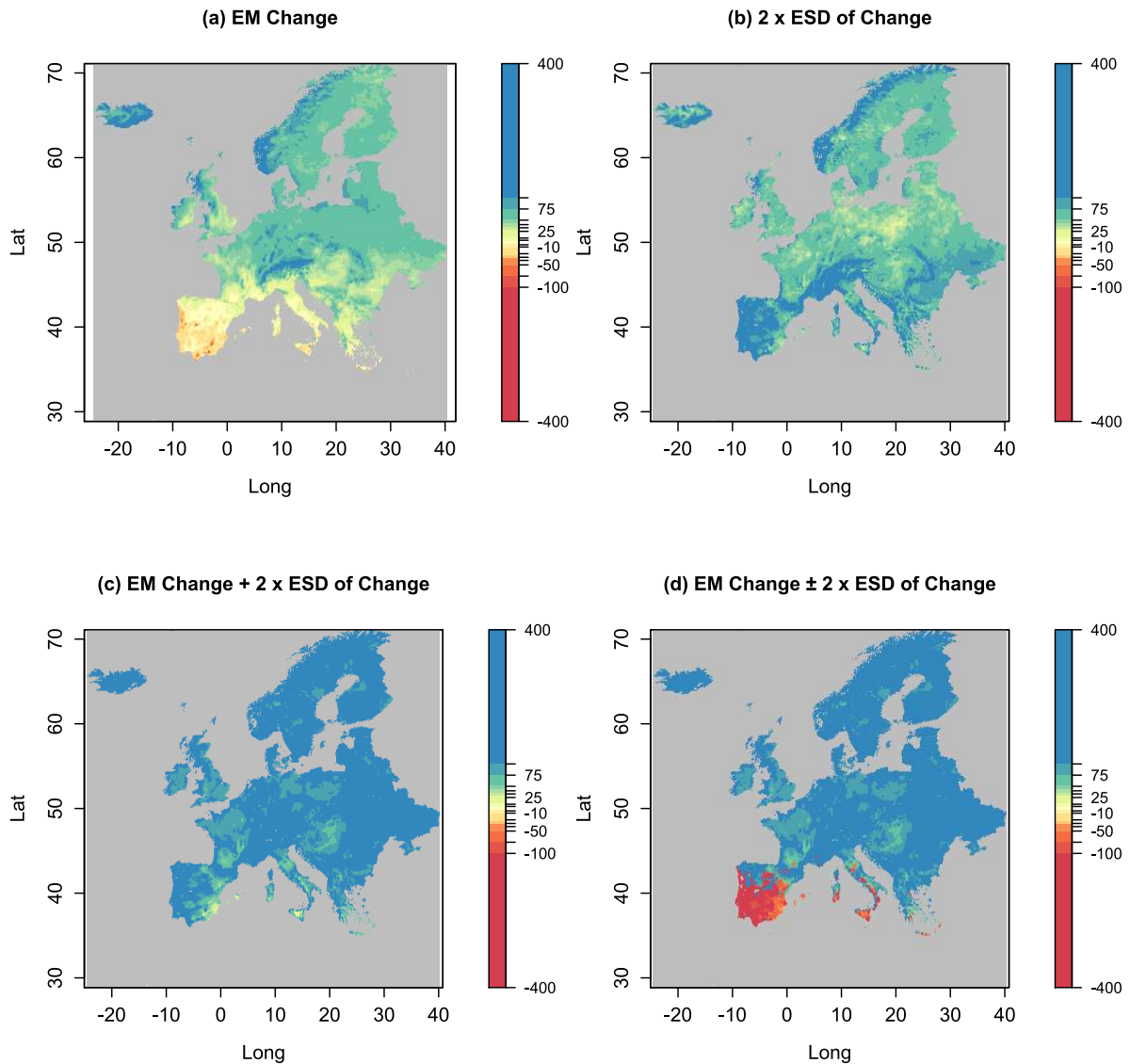
778 **Figure 4** Worst members and DCA patterns for 500 randomly generated ensembles, for the same parameters as
 779 the ensembles shown in Fig. 3. The red dots show the mean of the ensemble means. Panel (a) shows 500 worst
 780 members, one for each ensemble. Panel (b) shows 500 DCA patterns, one for each ensemble

781



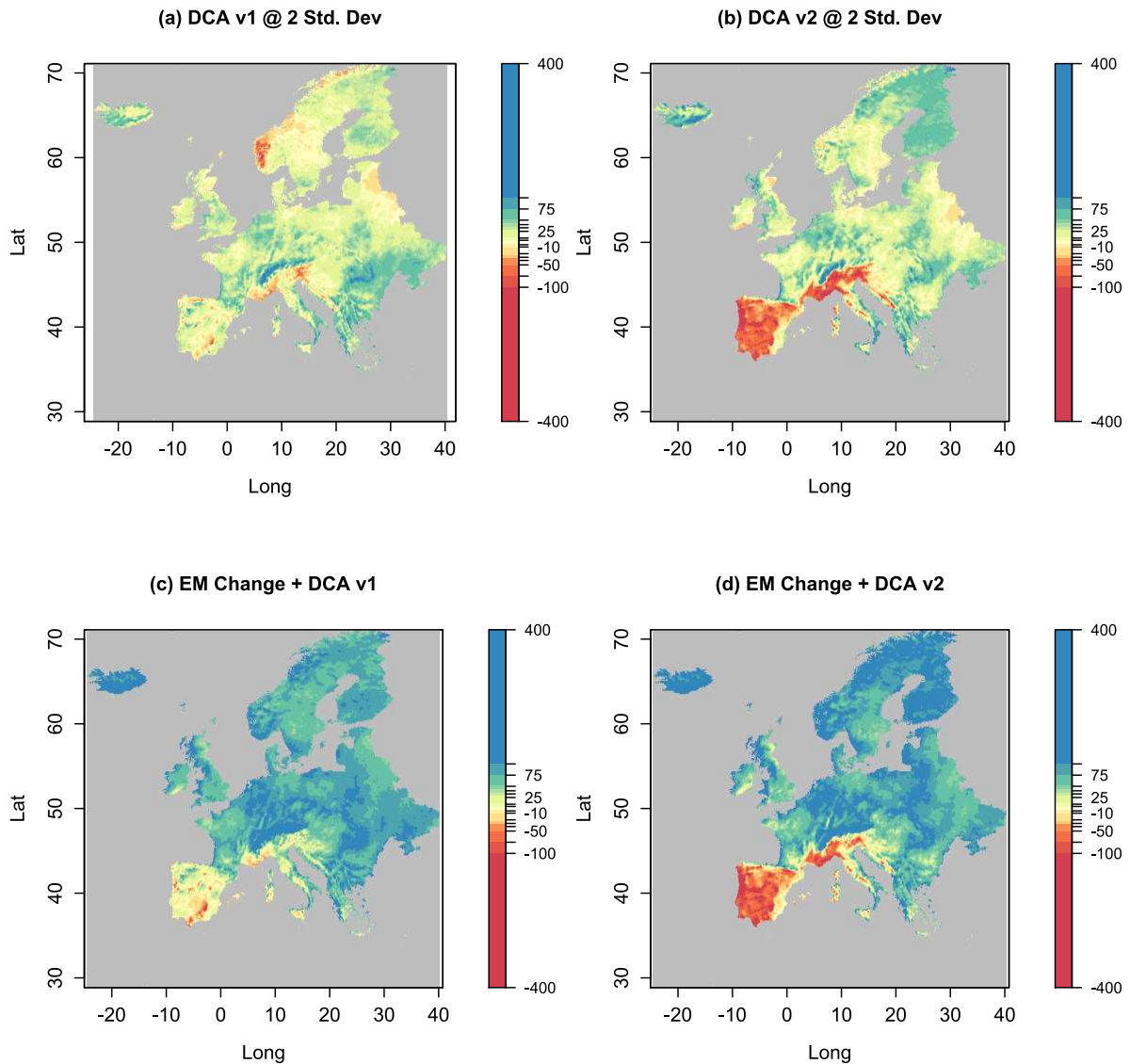
782

783 **Figure 5** Illustrations of mathematical properties of DCA. In each panel, the gradient of increasing impact is
 784 shown by the black arrow that points towards the top right hand corner. Panel (a) shows probability densities p
 785 for a bivariate normal, with darker shading indicating higher densities, but lower values of the Mahalanobis
 786 distance m from the origin. The density is elliptical, and the principal axis of the ellipse is given by the green
 787 arrow. Panel (b) shows values of a linear impact function a increasing towards the top right-hand corner, with
 788 darker shading indicating higher impact. Panel (c) shows the DCA pattern as a black cross, calculated using Eq.
 789 (1) with r normalized to unit length. This black cross is repeated in all subsequent panels. Panel (d) shows the
 790 DCA pattern as a red circle, calculated using Eq. (2). Panel (e) shows values of the ratio a'/m , with darker shading
 791 indicating higher values. Panel (f) shows values of the product pa' , with darker shading showing higher values.
 792 Panel (g) shows three examples of the conditional mean pattern, conditional on exceeding a certain level of impact,
 793 as red circles. The impact thresholds are given by the three diagonal lines. Panel (h) shows three examples of the
 794 impact-weighted conditional mean pattern as red circles, conditional on exceeding a certain level of impact. The
 795 impact thresholds are given by the diagonal lines. Panel (i) shows three examples of quadratic DCA patterns, as
 796 red circles



797

798 **Figure 6** Annual mean precipitation change from the EURO-CORDEX ensemble, based on the models listed in
 799 Table 1, for the difference between the periods 2011-2040 and 1981-2010, in mm/year. EM is ensemble mean and
 800 ESD is ensemble standard deviation. Panel (a) shows the ensemble mean change, panel (b) shows twice the
 801 standard deviation of change. Panel (c) shows the ensemble mean change plus twice the standard deviation of
 802 change and panel (d) shows the ensemble mean change plus twice the standard deviation of change in regions
 803 where the ensemble mean change is positive, and the ensemble mean change *minus* twice the standard deviation
 804 of change in regions where the ensemble mean change is negative. Non-linear colour scales are used to highlight
 805 the spatial variations



806

807 **Figure 7** Reasonable worst-case precipitation scenarios calculated using DCA, based on the EURO-CORDEX
 808 data used to create Fig. 6. Panel (a) shows a DCA pattern derived from an impact function defined as the sum of
 809 precipitation at all points, normalized to two standard deviations. Panel (c) shows the ensemble mean change plus
 810 this pattern. Panel (b) shows a DCA pattern derived from an impact function defined as the sum of precipitation
 811 at all points where the ensemble mean change shows positive precipitation, minus the sum of precipitation at all
 812 points where the ensemble mean change shows negative precipitation. Panel (d) shows the ensemble mean change
 813 plus this pattern

814

Figures

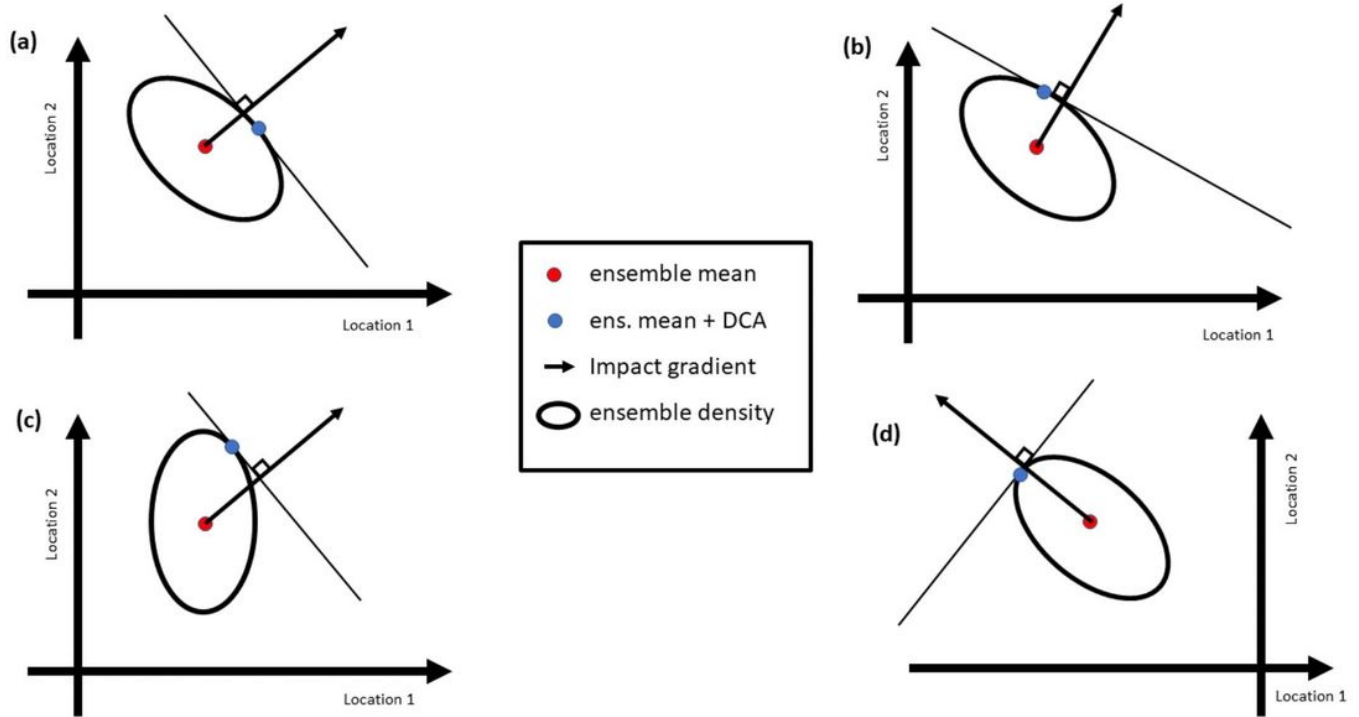


Figure 1

Four illustrations of Directional Component Analysis (DCA), applied to climate variables at locations 1 and locations 2. The ellipse in each case illustrates a contour of probability density for an ensemble prediction for these two locations. The ensemble is assumed to be bivariate normally distributed. The red dot in each case illustrates the ensemble mean, the arrow indicates the gradient of increasing impact, the straight line, which is perpendicular to the arrow, indicates a line of constant impact and the blue dot indicates the resulting DCA pattern. Examples (a) and (b) show the same ensemble, but different directions of impact, and hence different DCA patterns. Examples (a) and (c) show different ensembles, but the same direction of impact, and hence different DCA patterns. Example (d) shows a different ensemble and a new direction of impact

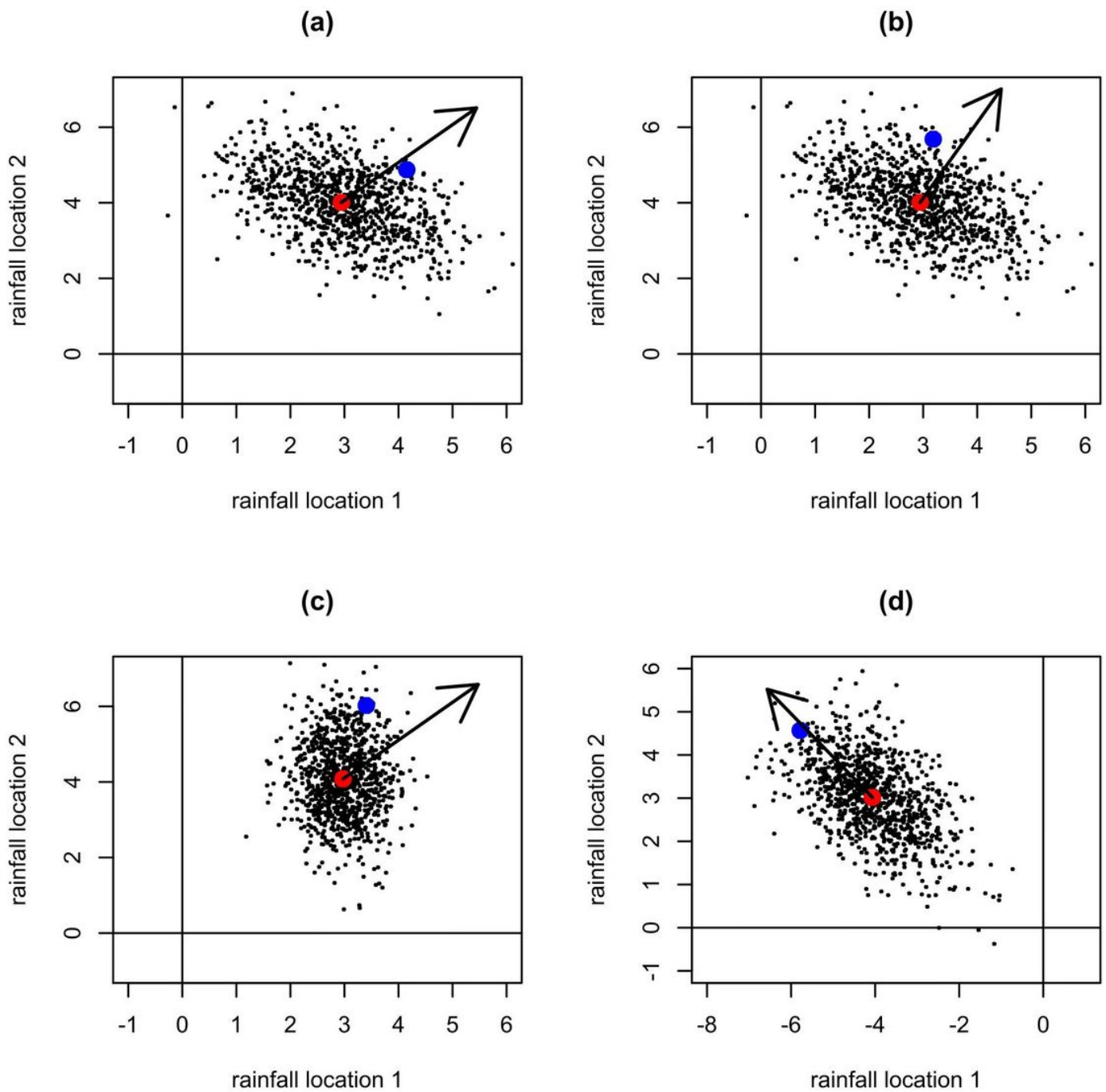


Figure 2

Four randomly generated 1000 member examples and related quantities. In each case the ensemble members are shown by black dots, the ensemble mean is shown by a red dot, the gradient of increasing impact is shown by the arrow and the ensemble mean plus the DCA pattern, scaled to two standard deviations of impact, is shown by a blue dot. Examples (a) and (b) use the same ensemble, while examples (a) and (c) use the same impact vector. These examples correspond to the illustrations in Fig. 1

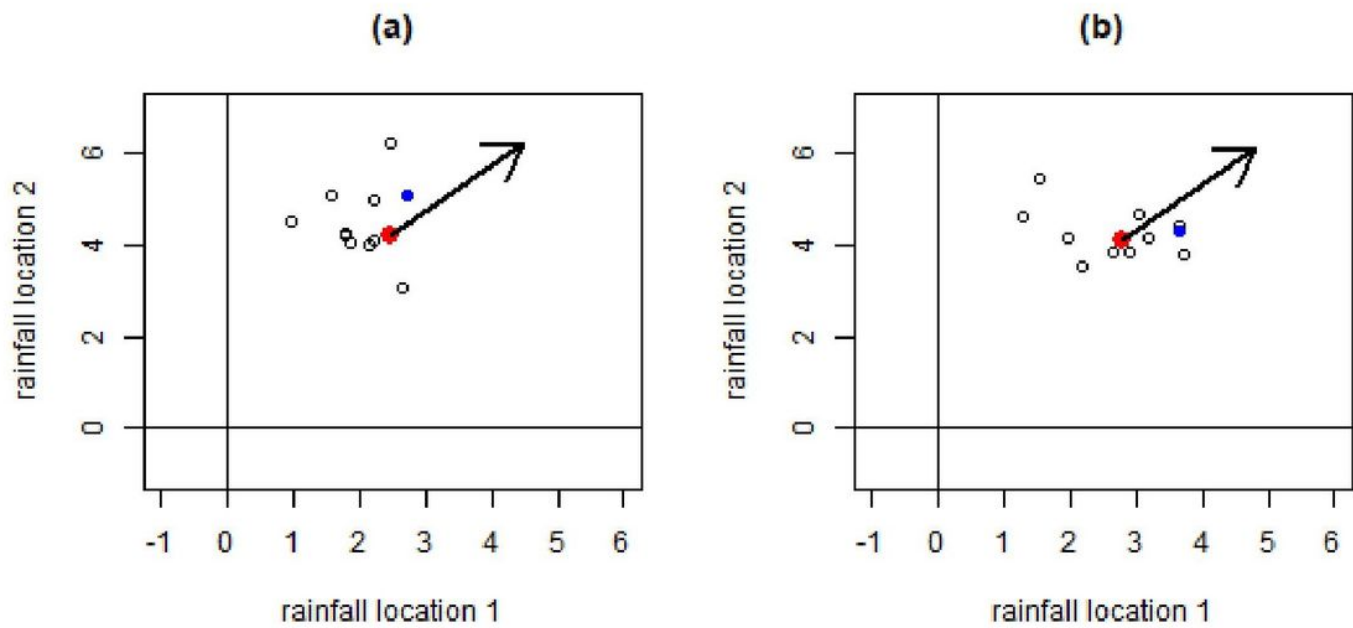


Figure 3

As Fig. 2a, but now for two randomly generated 10 member ensembles

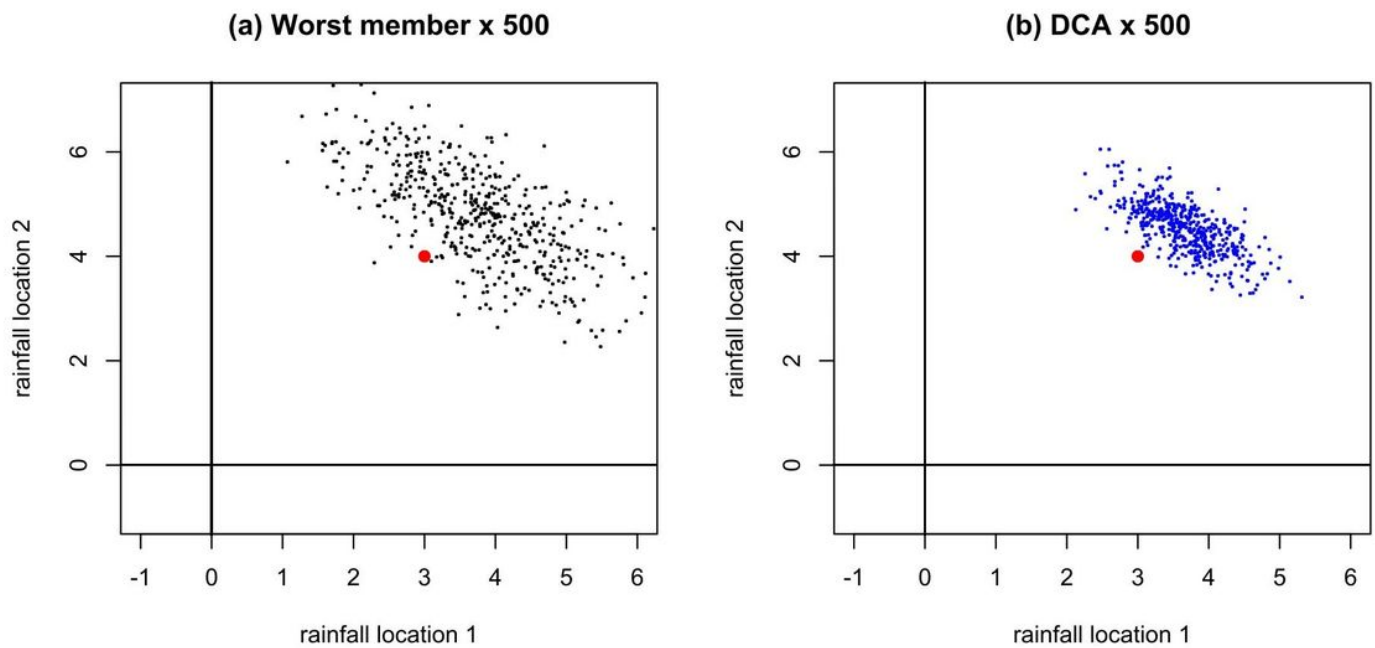


Figure 4

Worst members and DCA patterns for 500 randomly generated ensembles, for the same parameters as the ensembles shown in Fig. 3. The red dots show the mean of the ensemble means. Panel (a) shows 500 worst members, one for each ensemble. Panel (b) shows 500 DCA patterns, one for each ensemble

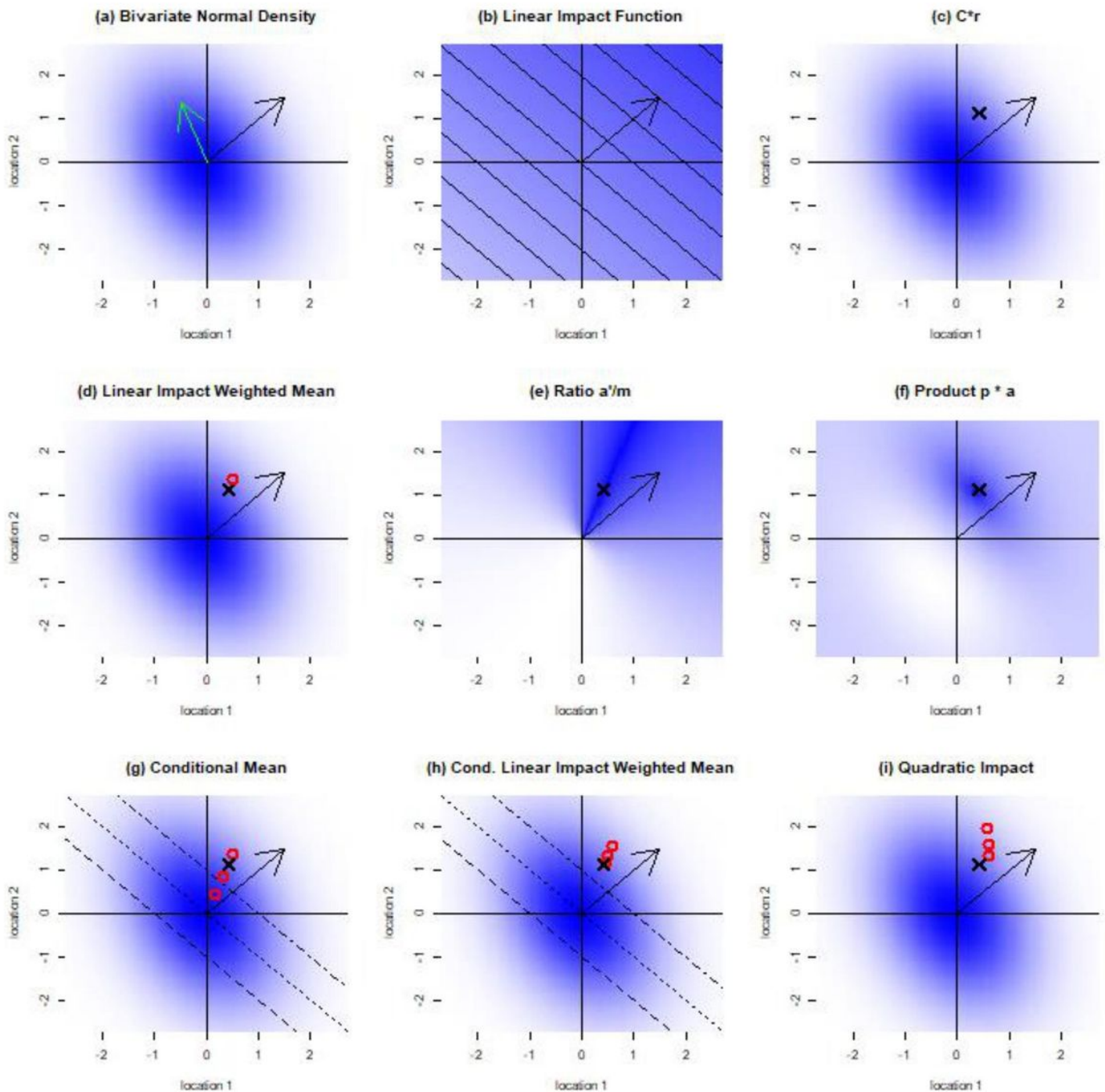


Figure 5

Illustrations of mathematical properties of DCA. In each panel, the gradient of increasing impact is shown by the black arrow that points towards the top right hand corner. Panel (a) shows probability densities φ for a bivariate normal, with darker shading indicating higher densities, but lower values of the Mahalanobis distance δ from the origin. The density is elliptical, and the principal axis of the ellipse is given by the green arrow. Panel (b) shows values of a linear impact function φ increasing towards the top right-hand corner, with darker shading indicating higher impact. Panel (c) shows the DCA pattern as a

black cross, calculated using Eq. (1) with $\hat{\mu}$ normalized to unit length. This black cross is repeated in all subsequent panels. Panel (d) shows the DCA pattern as a red circle, calculated using Eq. (2). Panel (e) shows values of the ratio $\hat{\mu}'/\hat{\mu}$, with darker shading indicating higher values. Panel (f) shows values of the product $\hat{\mu}\hat{\mu}'$, with darker shading showing higher values. Panel (g) shows three examples of the conditional mean pattern, conditional on exceeding a certain level of impact, as red circles. The impact thresholds are given by the three diagonal lines. Panel (h) shows three examples of the impact-weighted conditional mean pattern as red circles, conditional on exceeding a certain level of impact. The impact thresholds are given by the diagonal lines. Panel (f) shows three examples of quadratic DCA patterns, as red circles

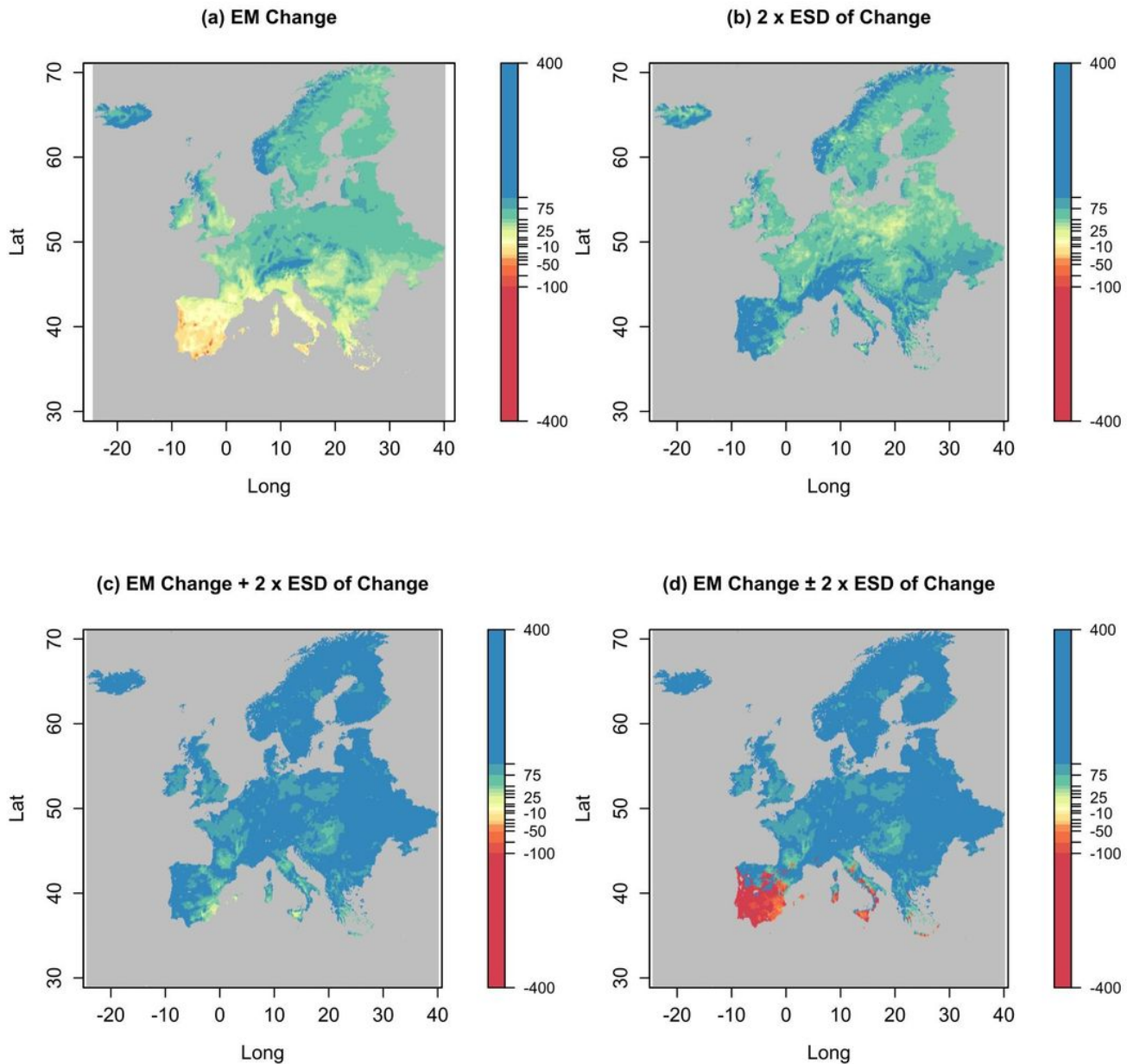


Figure 6

Annual mean precipitation change from the EURO-CORDEX ensemble, based on the models listed in Table 1, for the difference between the periods 2011-2040 and 1981-2010, in mm/year. EM is ensemble mean and ESD is ensemble standard deviation. Panel (a) shows the ensemble mean change, panel (b) shows twice the standard deviation of change. Panel (c) shows the ensemble mean change plus twice the standard deviation of change and panel (d) shows the ensemble mean change plus twice the standard deviation of change in regions where the ensemble mean change is positive, and the ensemble mean change minus twice the standard deviation of change in regions where the ensemble mean change is negative. Non-linear colour scales are used to highlight the spatial variations Note: The designations employed and the presentation of the material on this map do not imply the expression of any opinion whatsoever on the part of Research Square concerning the legal status of any country, territory, city or area or of its authorities, or concerning the delimitation of its frontiers or boundaries. This map has been provided by the authors.

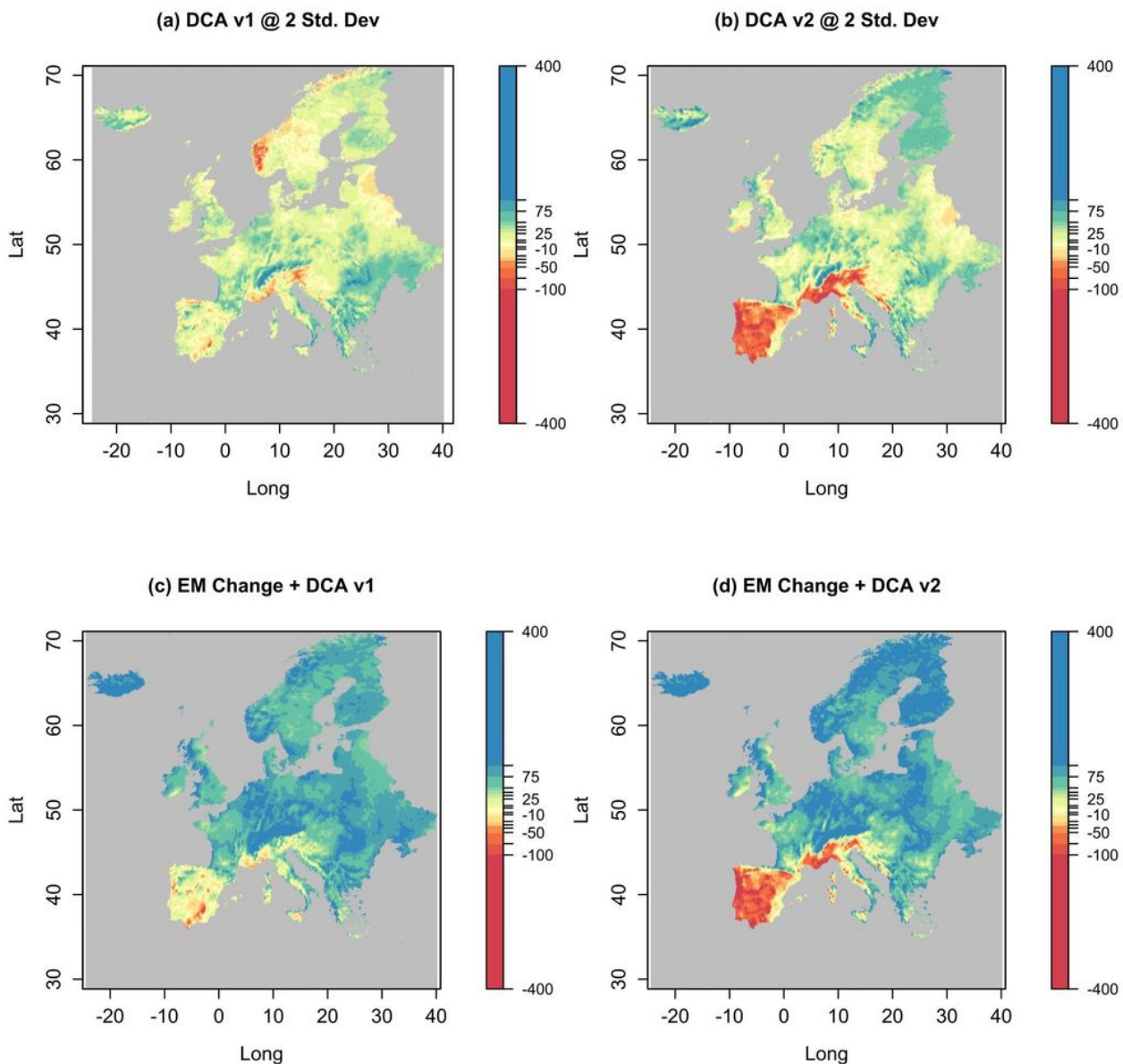


Figure 7

Reasonable worst-case precipitation scenarios calculated using DCA, based on the EURO-CORDEX data used to create Fig. 6. Panel (a) shows a DCA pattern derived from an impact function defined as the sum of precipitation at all points, normalized to two standard deviations. Panel (c) shows the ensemble mean change plus this pattern. Panel (b) shows a DCA pattern derived from an impact function defined as the sum of precipitation at all points where the ensemble mean change shows positive precipitation, minus the sum of precipitation at all points where the ensemble mean change shows negative precipitation. Panel (d) shows the ensemble mean change plus this pattern. Note: The designations employed and the presentation of the material on this map do not imply the expression of any opinion whatsoever on the part of Research Square concerning the legal status of any country, territory, city or area or of its authorities, or concerning the delimitation of its frontiers or boundaries. This map has been provided by the authors.